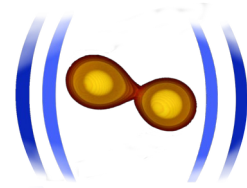




European Research Council
Established by the European Commission

DFG

Deutsche
Forschungsgemeinschaft



www.computational-relativity.org

Modeling the strong-field dynamics of binary neutron star mergers

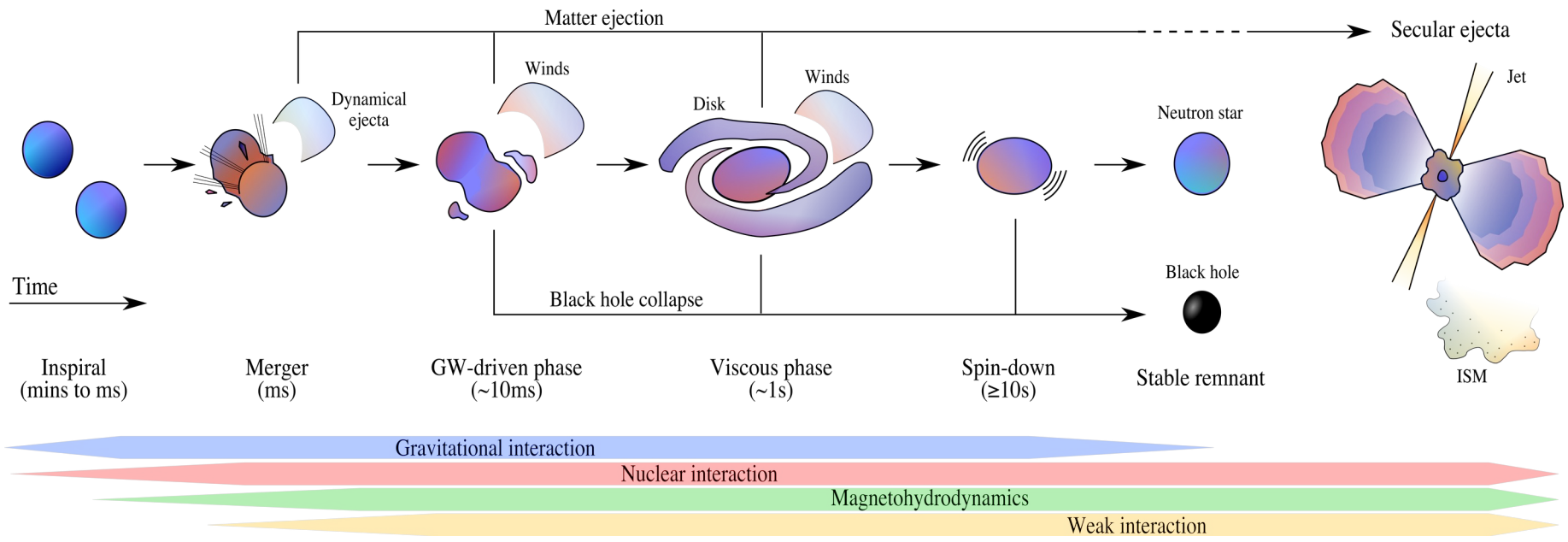
S. Bernuzzi



**FRIEDRICH-SCHILLER-
UNIVERSITÄT
JENA**

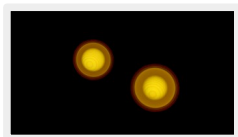
Einstein Toolkit Workshop – July 2024

The picture emerging from theory

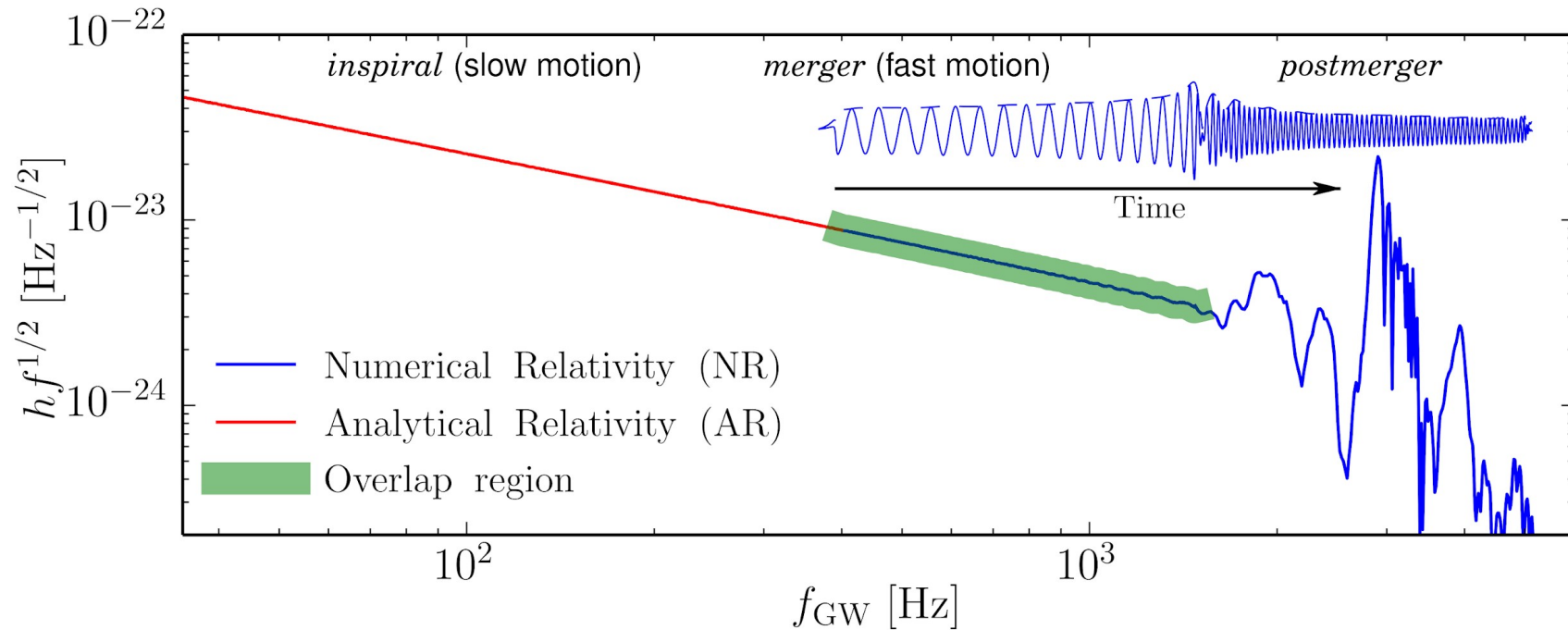
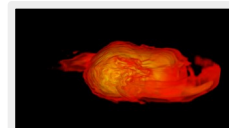
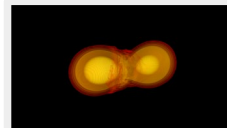


Gravitational waves

The complete GW spectrum



SB+ [<https://arxiv.org/abs/1504.01764>]
Breschi,SB+ [<https://arxiv.org/abs/1908.11418>]
Breschi,SB+ [<https://arxiv.org/abs/2205.09112>]



Measurability of the tidal polarizability of neutron stars in late-inspiral gravitational-wave signals

Thibault Damour and Alessandro Nagar

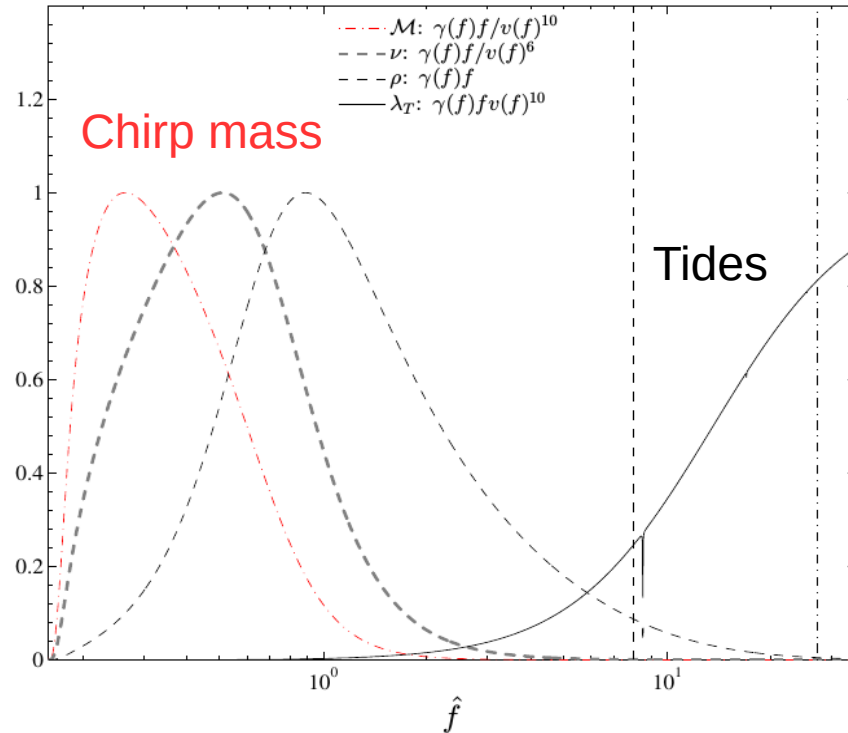
Institut des Hautes Etudes Scientifiques, 91440 Bures-sur-Yvette, France ICRANet, 65122 Pescara, Italy

Loïc Villain

Laboratoire de Mathématiques et de Physique Théorique, Univ. F. Rabelais—CNRS (UMR 7350),

Féd. Denis Poisson, 37200 Tours, France

(Received 20 March 2012; published 15 June 2012)



Systematics & waveform accuracy

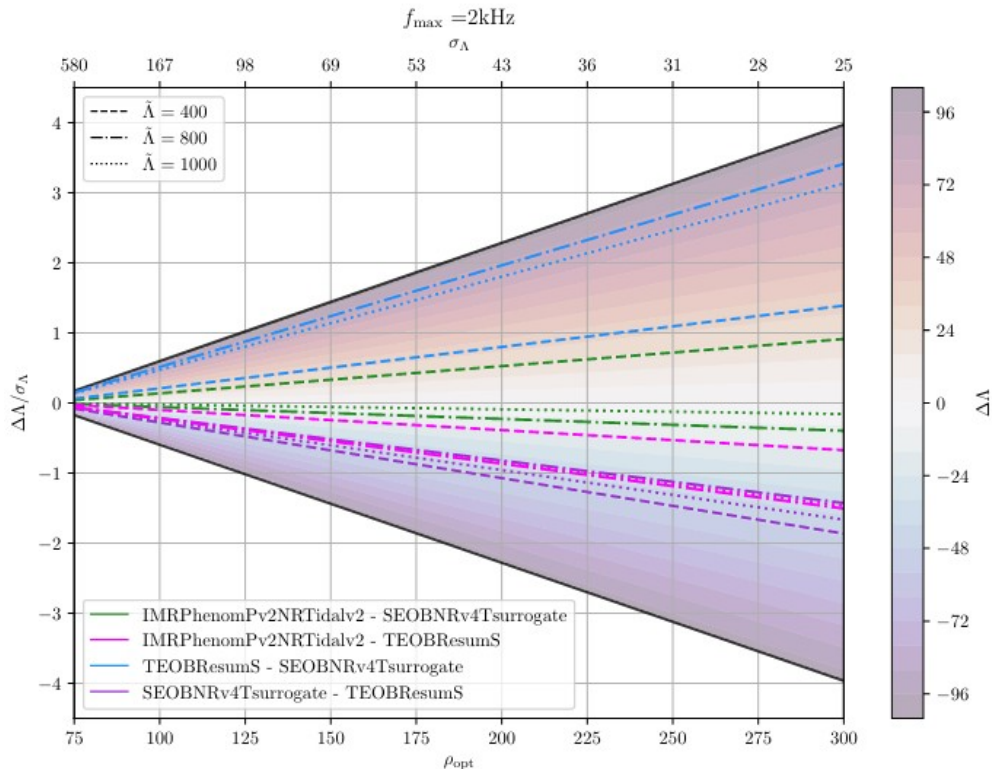
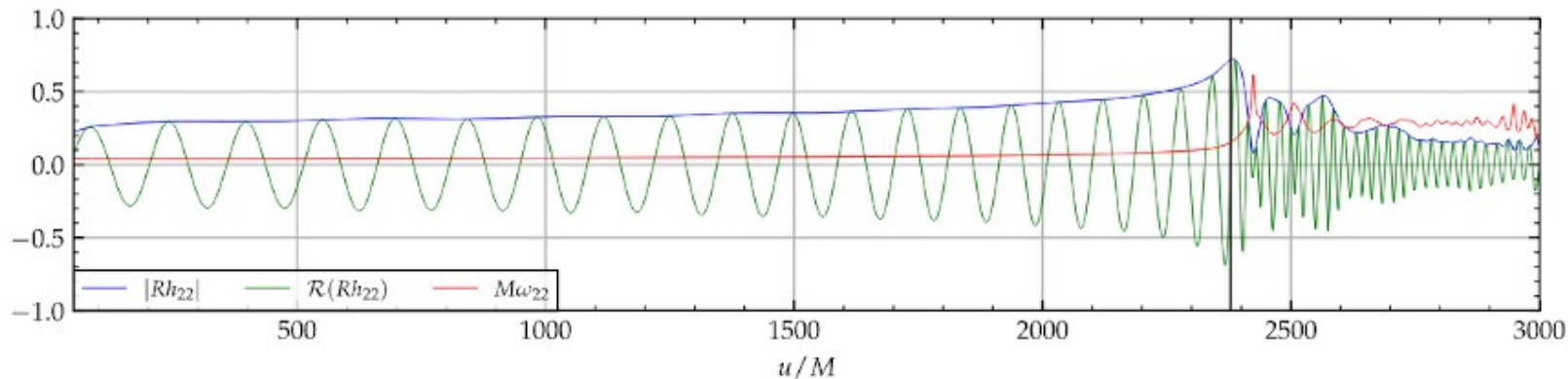
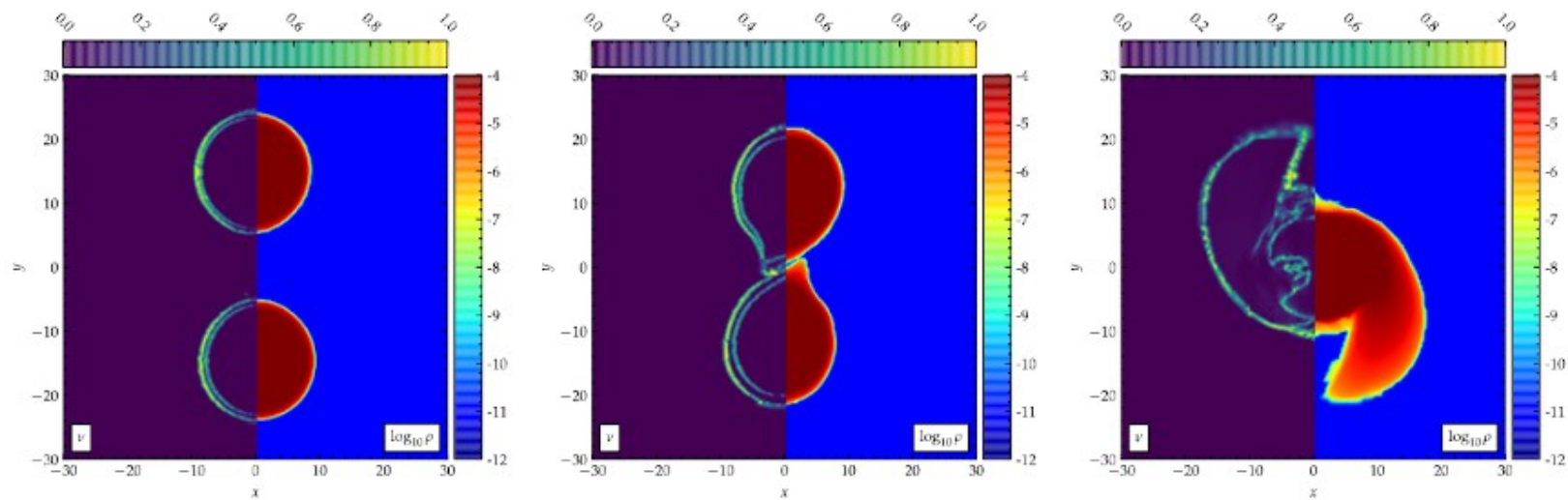


TABLE V. Faithfulness values \mathcal{F} computed considering frequencies from f_{low} to $f_{\text{mr}}g$ between simulations with the same intrinsic parameters and two different resolutions, extracted at $r/M = 1000$. The source is situated in the same sky location as GW170817, and the waveform polarizations h_+ and h_{\times} are computed and projected on the Livingston detector. We employ the `aLIGODesignSensitivityP1200087` [22] PSD from `pycbc` [10] to compute the matches, and compare the values obtained to the thresholds \mathcal{F}_{thr} calculated with Eq. 19 with $\epsilon^2 = 1$ or $\epsilon^2 = N$. A tick \checkmark indicates that $\mathcal{F} > \mathcal{F}_{\text{thr}}$. Conversely, a cross \times indicates that $\mathcal{F} < \mathcal{F}_{\text{thr}}$.

Sim	r^a	\mathcal{F}	SNR						
			14		30		80		
			$N = 6$	1	$N = 6$	1	$N = 6$	1	
BAM:0011	[96, 64]	0.991298	\checkmark	\times	\times	\times	\times	\times	\times
BAM:0017	[96, 64]	0.985917	\checkmark	\times	\times	\times	\times	\times	\times
BAM:0021	[96, 64]	0.957098	\times	\times	\times	\times	\times	\times	\times
BAM:0037	[216, 144]	0.998790	\checkmark	\checkmark	\checkmark	\times	\times	\times	\times
BAM:0048	[108, 72]	0.983724	\times	\times	\times	\times	\times	\times	\times
BAM:0058	[64, 64]	0.999127	\checkmark	\checkmark	\checkmark	\times	\times	\times	\times
BAM:0064	[240, 160]	0.997427	\checkmark	\times	\checkmark	\times	\times	\times	\times
BAM:0091	[144, 108]	0.997810	\checkmark	\checkmark	\checkmark	\times	\times	\times	\times
BAM:0094	[144, 108]	0.996804	\checkmark	\times	\checkmark	\times	\times	\times	\times
BAM:0095	[256, 192]	0.999550	\checkmark	\checkmark	\checkmark	\checkmark	\checkmark	\checkmark	\times
BAM:0107	[128, 96]	0.995219	\checkmark	\times	\times	\times	\times	\times	\times
BAM:0127	[128, 96]	0.999011	\checkmark	\checkmark	\checkmark	\times	\times	\times	\times

^a Number of grid point (linear resolution) of the finest grid refinement, roughly covering the diameter of one NS

Main issue for tidal parameters inference!



Entropy flux-limiter scheme

Doulis, Atteneder, SB, Bruegmann [<https://arxiv.org/abs/2202.08839>] (see also previous work by Guercilena+)

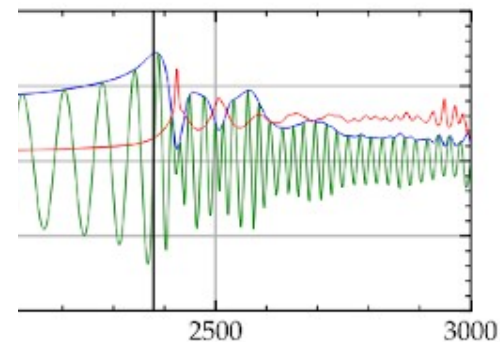
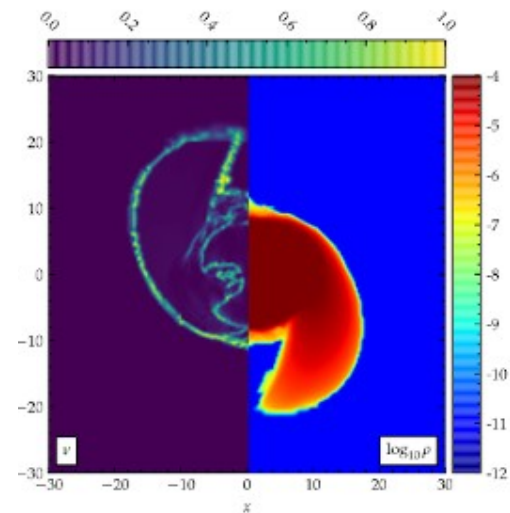
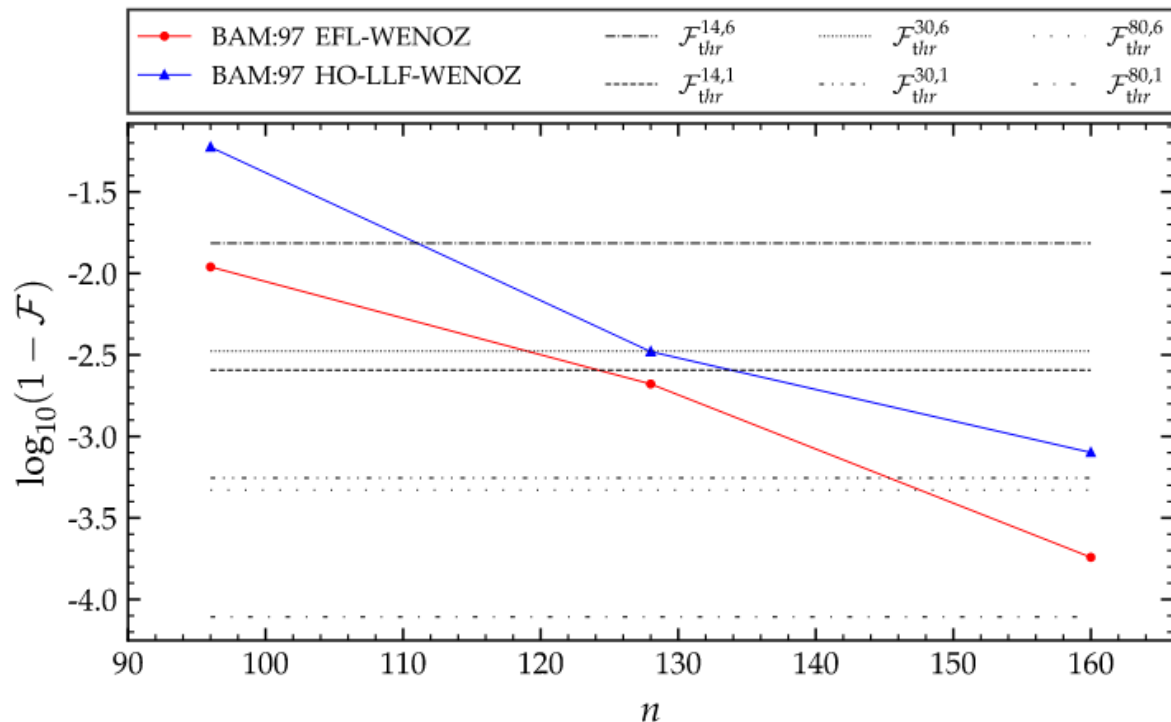


FIG. 21. Faithfulness as a function of the resolution for the BAM:97 simulation.

Entropy flux-limiter scheme

Doulis,Atteneder,SB,Bruegmann [<https://arxiv.org/abs/2202.08839>] (see also previous work by Guercilena+)

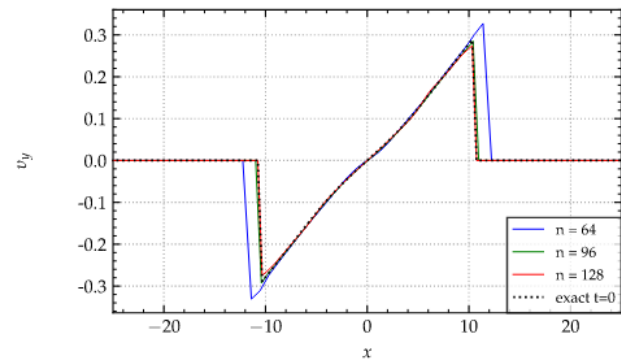
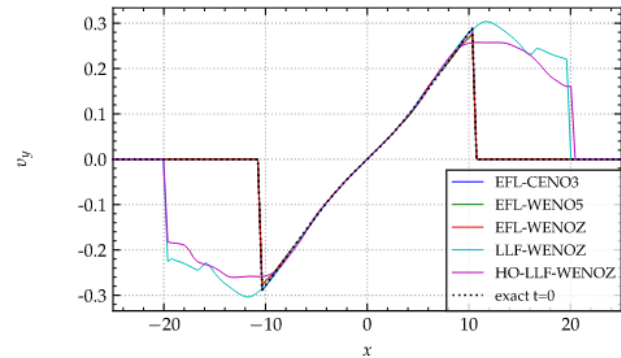
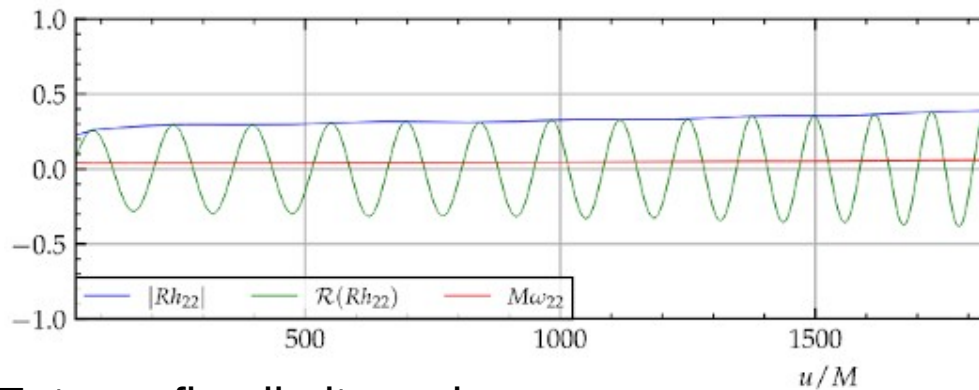
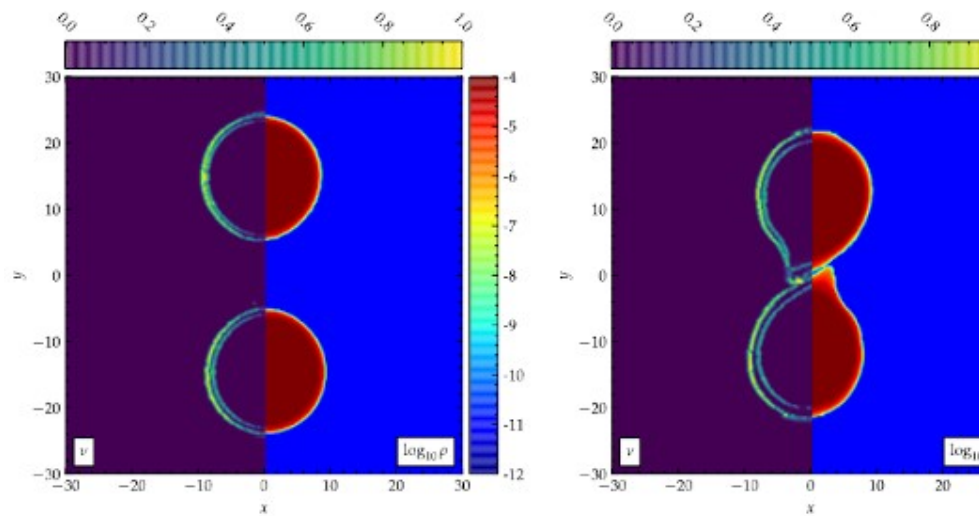


FIG. 9. Velocity profile of a stationary rotating neutron star in a dynamical spacetime with Γ -law EoS. Top: One-dimensional profile of the velocity component v_y along the x -direction at time $t = 1000$ (four periods) with $n = 128$. Bottom: The v_y profile of the WENO5 scheme with increasing resolution.

Entropy flux-limiter scheme

Doulis, Atteder, SB, Bruegmann [<https://arxiv.org/abs/2202.08839>]

KiloHertz spectrum (remnant emission)

PRL 115, 091101 (2015)

PHYSICAL REVIEW LETTERS

week ending
28 AUGUST 2015

Modeling the Complete Gravitational Wave Spectrum of Neutron Star Mergers

Sebastiano Bernuzzi,^{1,2} Tim Dietrich,³ and Alessandro Nagar⁴

¹TAPIR, California Institute of Technology, 1200 East California Boulevard, Pasadena, California 91125, USA

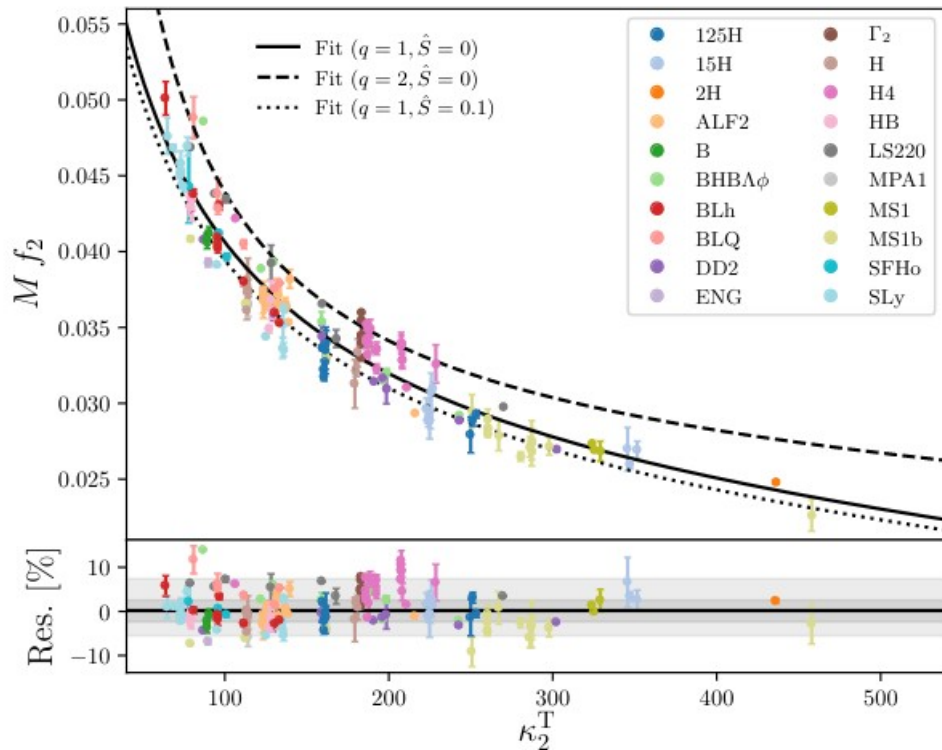
²DiFeST, University of Parma and INFN Parma, I-43124 Parma, Italy

³Theoretical Physics Institute, University of Jena, 07743 Jena, Germany

⁴Institut des Hautes Etudes Scientifiques, 91440 Bures-sur-Yvette, France

(Received 9 April 2015; revised manuscript received 11 June 2015; published 27 August 2015)

- Quasiuniversal (EOS-insensitive) relations w/ tidal coupling constant
SB+ [<https://arxiv.org/abs/1504.01764>]
- First complete spectrum model (EOB completion with NRPM)
Breschi+ [<https://arxiv.org/abs/1908.11418>]
- Improved frequency domain NRPMw
Breschi+ [<https://arxiv.org/abs/2205.09112>]



Full-spectrum constraints on M-R diagram

- Full-spectrum (mock) analysis using ET @ minimum SNR threshold for a PM detection
- NS maximum density to 15% and maximum mass to 12% (90% C.L.) using direct quasiuniversal relation
- Hits theoretical uncertainty, i.e. not possible to do better
- **Recalibration parameters:** account for theoretical uncertainties in EOS-insensitive rel.

Breschi, SB+ [<https://arxiv.org/abs/2110.06957>]

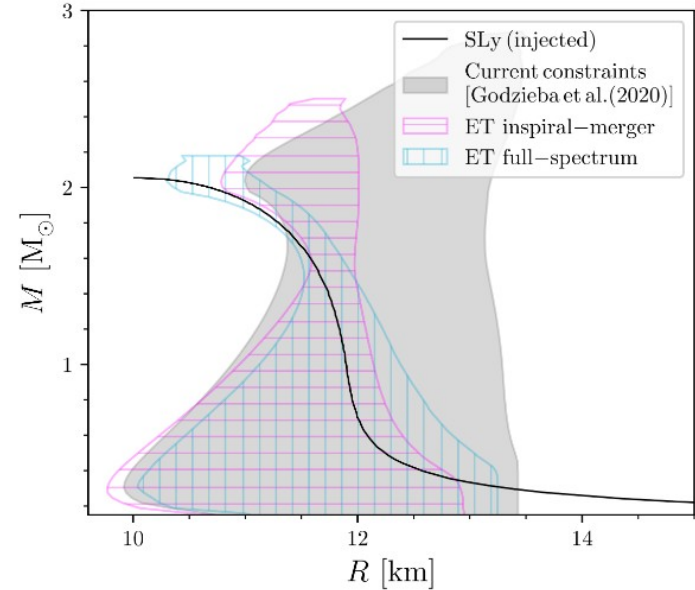
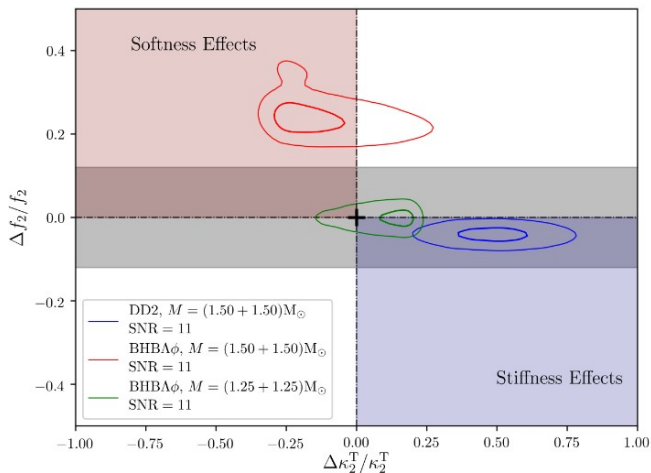
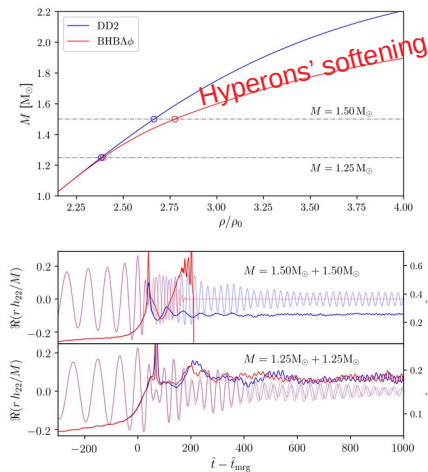


FIG. 4. Mass-radius diagram constraints from a single full-spectrum Einstein Telescope (ET) BNS observation with PM SNR 10 (total SNR 180). The gray area (prior) corresponds to the two-million EOS sample of Ref. [69]. The magenta and cyan areas are the 90% credibility regions given by inspiral-merger and inspiral-merger-PM inferences respectively. The full-spectrum (cyan) posterior agrees with the injected EOS (black).

3G/Einstein Telescope sensitivity to kHz GWs



“EOS Softness” (Hyperons, phase transitions,...)

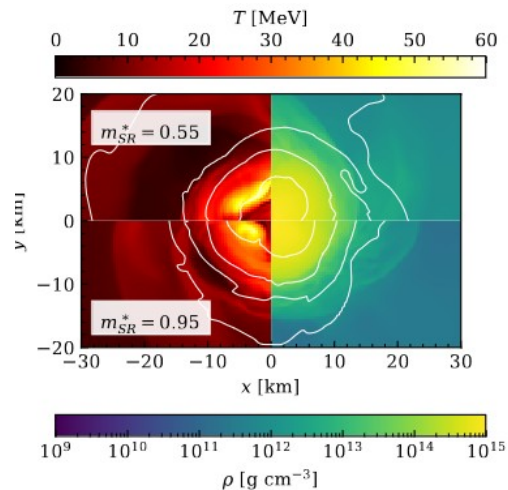
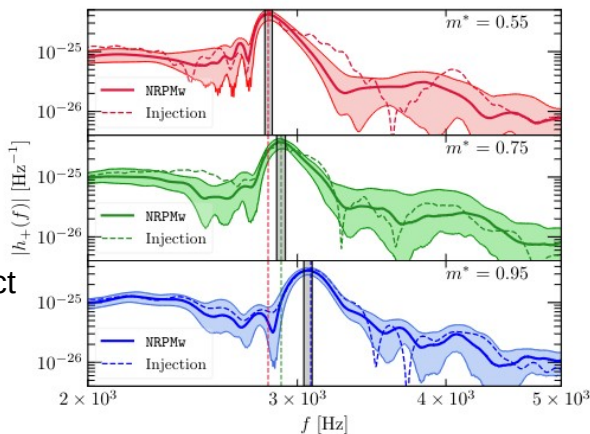
Effect of hyperonic d.o.f. at remnant densities:
 → pressure support reduces w.r.t hadronic
 → more compact remnant or black hole formation

Radice, SB+ [<https://arxiv.org/abs/1612.06429>]
 Breschi, SB+ [<https://arxiv.org/abs/1908.11418>]
 Breschi+ [<https://arxiv.org/abs/2301.09672>]

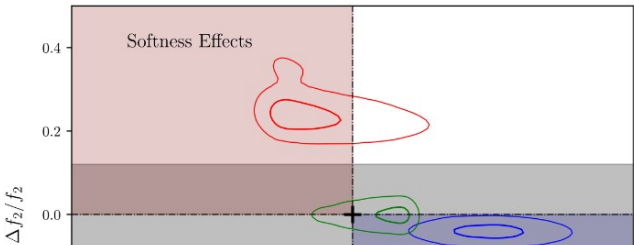
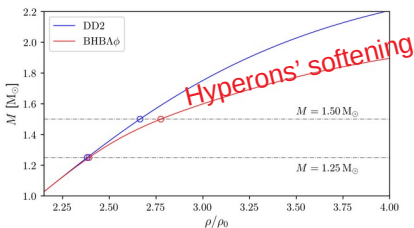
“Thermal effects” (effective nucleon mass)

Increasing effective nucleon mass:
 → specific heat increases
 → thermal pressure support reduces
 → the remnants become colder and more compact

Fields+ [<https://arxiv.org/abs/2302.11359>]

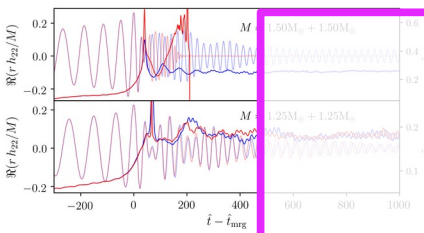


3G/Einstein Telescope sensitivity to kHz GWs



“EOS Softness” (Hyperons, phase transitions,...)

Effect of hyperonic d.o.f. at remnant densities:
 → pressure support reduces w.r.t hadronic
 → more compact remnant or black hole formation



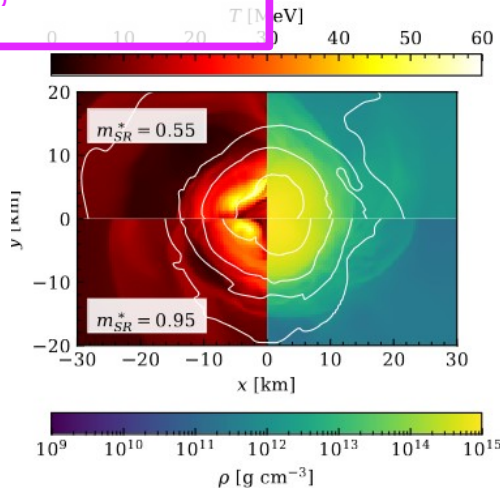
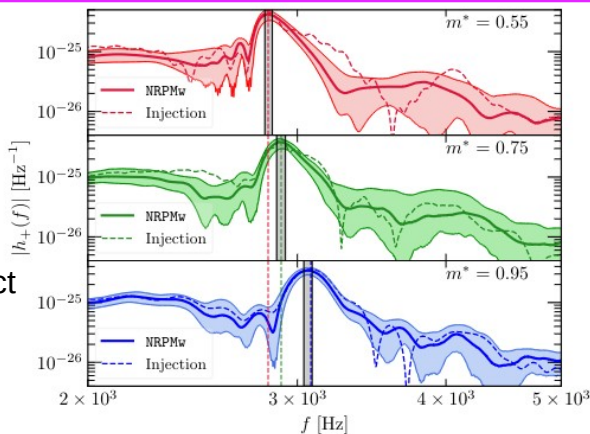
How to actually detect this?
 Would like unambiguous procedure ... but
 Quasi-universal relations, Degeneracies, ...

Radice, SB+ [<https://arxiv.org/abs/1612.06429>]
 Giacomini, SB+ [<https://arxiv.org/abs/1908.11418>]
 Breschi+ [<https://arxiv.org/abs/2301.09672>]

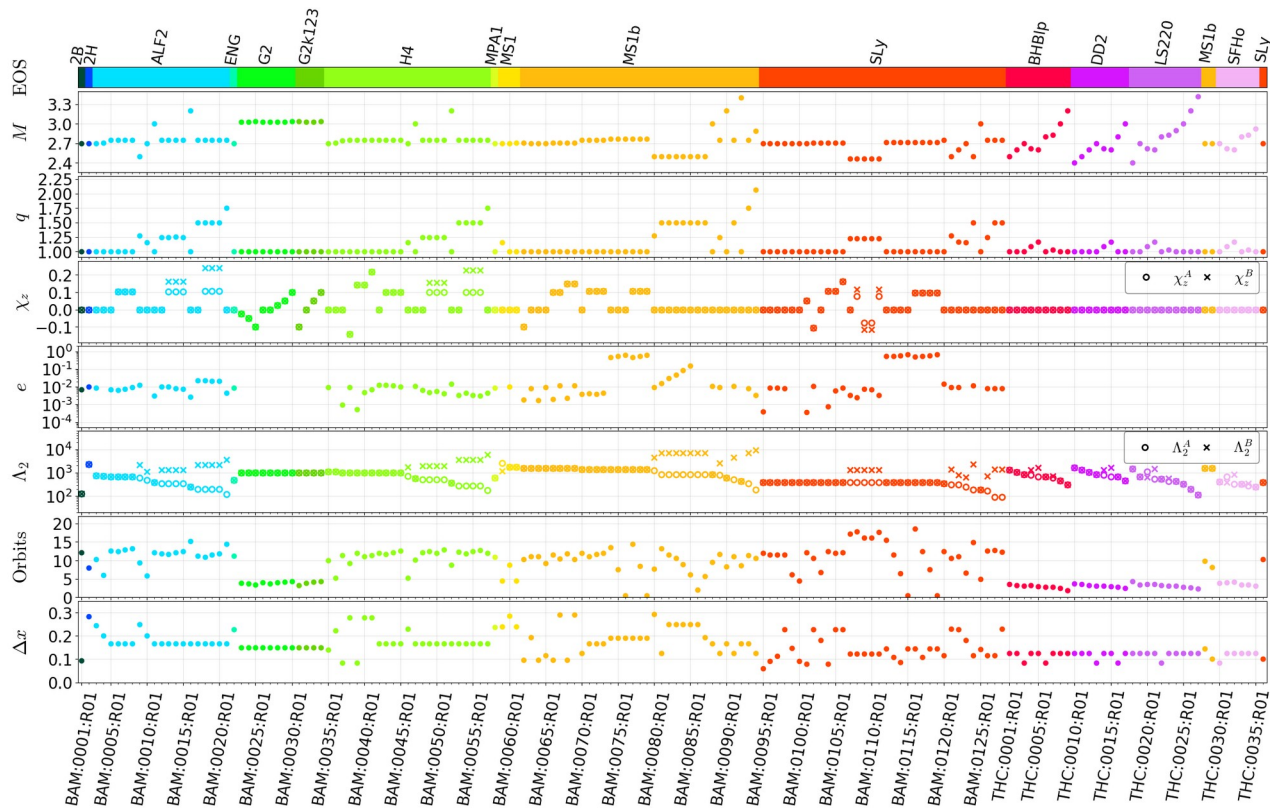
“Thermal effects” (effective nucleon mass)

Increasing effective nucleon mass:
 → specific heat increases
 → thermal pressure support reduces
 → the remnants become colder and more compact

Fields+ [<https://arxiv.org/abs/2302.11359>]



Public data release



NR-GW OpenData

Recent uploads

Search NR-GW OpenData

April 19, 2021 (v1) [Journal article](#) [Open Access](#)

Dynamical ejecta synchrotron emission as a possible contributor to the rebrightening of GRB170817A

Nedora, Vsevolod Radice, David Bernuzzi, Sebastiano Perego, Albino, Daszuta, Boris Endrizzi, Andrea Prakash, Aviral Schianchi, Federico

Dynamical ejecta synchrotron emission as a possible contributor to the rebrightening of GRB170817A Nedora, Vsevolod; Radice, David; Bernuzzi, Sebastiano; Perego, Albino; Daszuta, Boris; Endrizzi, Andrea; Prakash, Aviral; Schianchi, Federico. We release light curves of the synchrotron emission of d

Uploaded on April 19, 2021

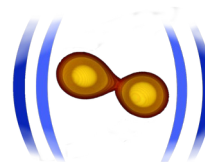
February 1, 2021 (v1) [Journal article](#) [Open Access](#)

Fast, faithful, frequency-domain effective-one-body waveforms for compact binary coalescences

Gamba, Rossella Bernuzzi, Sebastiano, Nagar, Alessandro

We release the data and the scripts used to produce the figures and tables of [1]. We additionally release a handful of scripts which may be used to reproduce our results (see README.md). TEOBResumSPA [1] is a frequency-domain effective-one-body multipolar approximant valid from any low frequency t

Uploaded on February 1, 2021



From remnants to kilonovae

Black-hole prompt collapse (equal masses)

$$M_{\text{collapse}} = k M_{\text{max}}^{\text{TOV}}$$

$$1.3 \lesssim k(\text{EOS}, C) \lesssim 1.7$$

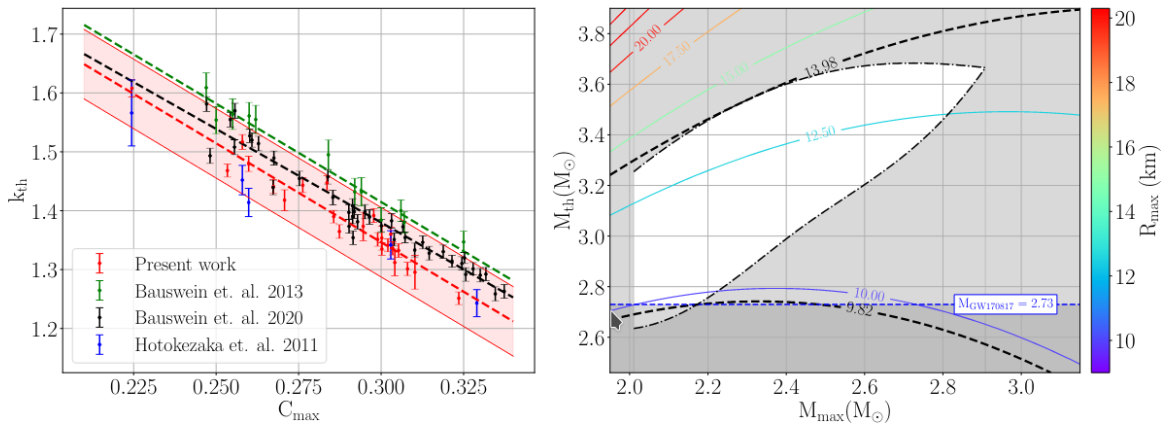
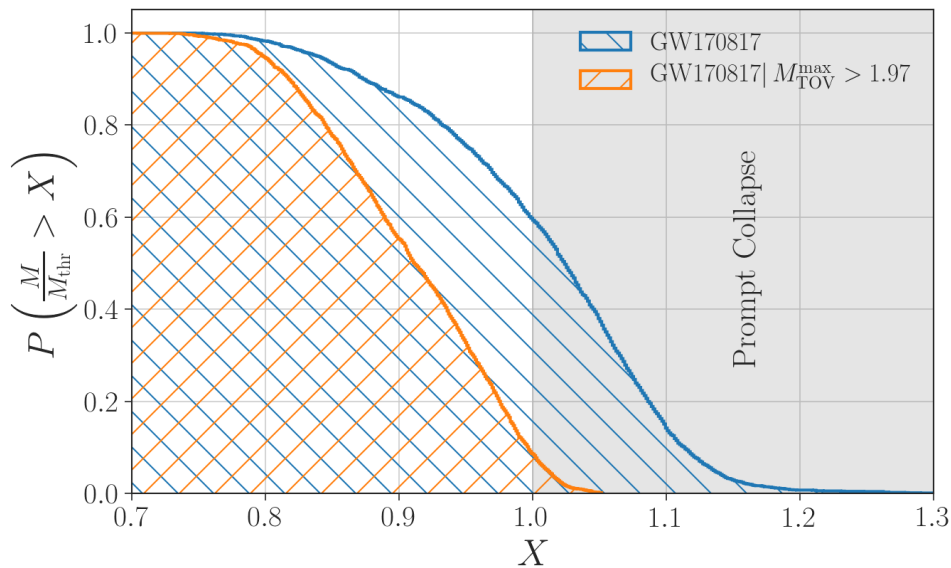


FIG. 4: *Left panel:* Plot of k_{th} vs. C_{max} from present and previous works [11, 18, 22]. Fits are constructed using our data and are shown in combination with the data of Hotokezaka *et al.* [11], Bauswein *et al.* [18] and Bauswein *et al.* [22]. The weighted linear regression results take into account the uncertainty in k_{th} . The shaded region represents uncertainties in the intercept. *Right panel:* Constraints on the R_{max} , M_{max} and M_{th} obtained using the correlation in left panel, PWP phenomenological constraints in combination with the observational lower limit on the maximum mass of nonrotating neutron stars and total mass of the event GW170817 as the lowest limit for prompt collapse.

EOS-insensitive phenomenological relations linking collapse threshold mass to non-rotating NS max mass Hotokezaka+ [https://arxiv.org/abs/1105.4370], Bauswein+ [https://arxiv.org/abs/1307.5191]. Kashyap+ [https://arxiv.org/abs/2111.05183]

Constraints on maximum mass if prompt collapse if observationally established (e.g. via model selection); e.g. Kashyap+ [https://arxiv.org/abs/2111.05183] results in figure

Inferring prompt collapse from inspiral GW



$P_{\text{GW170817}}(\text{prompt collapse} | M < 1.97) < 10\%$

- Two methods, w/ NR-based PC criteria (consistent results)
 - EOS inference + Threshold mass
 - Tidal parameter + $\bar{\Lambda}$ -Threshold
- GW170817: quantitatively support the “mainstream” interpretation of counterparts

Margalit&Metzger [<https://arxiv.org/abs/1710.05938>]

- GW190425 ($M \sim 3.4 M_{\odot}$):

$P_{\text{GW190425}}(\text{prompt collapse}) \sim 97\%$

LVC [<https://arxiv.org/abs/2001.01761>]

Black-hole prompt collapse (unequal masses)

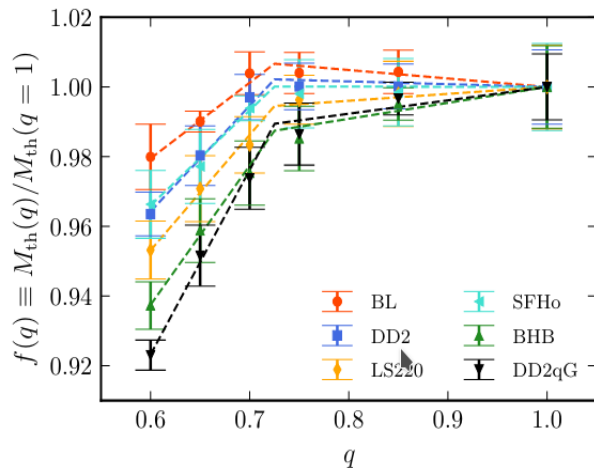
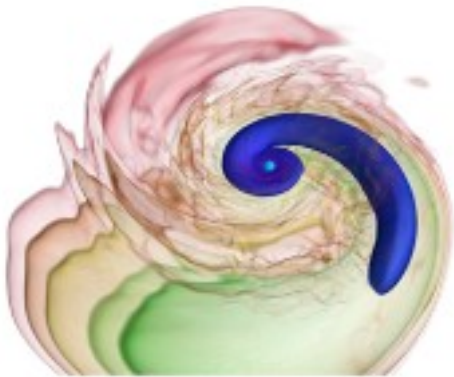


FIG. 2. Threshold PC masses normalized to the $q = 1$ case as a function of q for all the EOS used in this work. Dashed lines correspond to Eq. (2) fit.

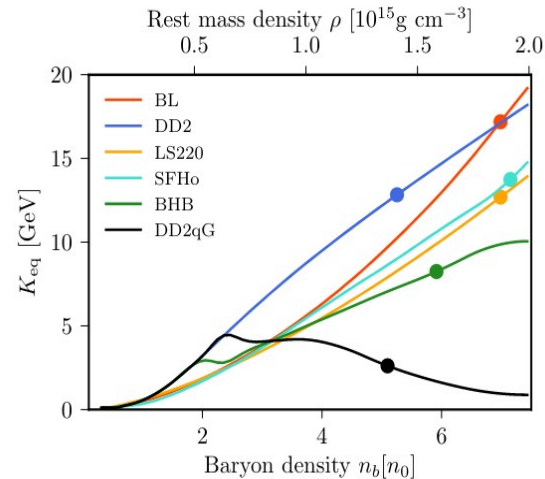


FIG. 1. Nuclear incompressibility K_{eq} of cold, β -equilibrated nuclear matter as a function of baryon density for the EOS employed in this work. Solid markers correspond to K_{max} , i.e. K_{eq} at the central density of the heaviest, irrotational NS.

Accretion-induced prompt collapse: tidal disruption and massive disks \rightarrow EM loud!
SB+ [<https://arxiv.org/abs/2003.06015>]

Collapse threshold depends Nuclear incompressibility of matter at max densities
Perego+ [<https://arxiv.org/abs/2112.05864>]

Trapped neutrinos and out-of-equilibrium effects

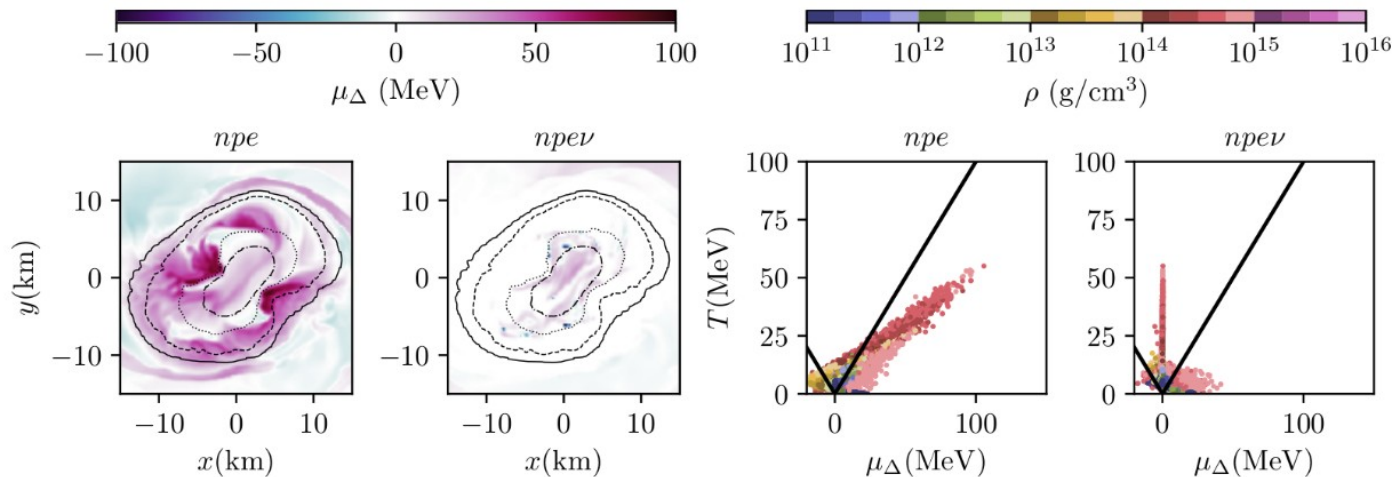
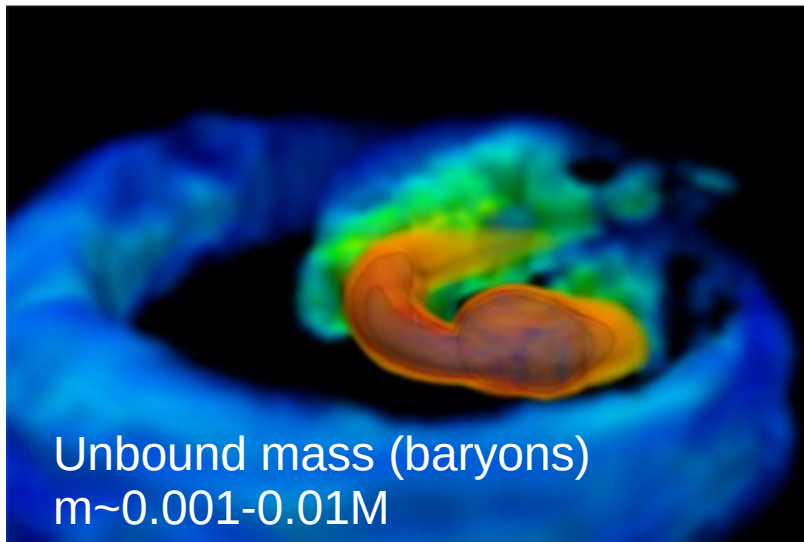


FIG. 1. *Left:* Equatorial snapshots of the out-of-equilibrium chemical potential μ_Δ at a time after the merger of $\delta t \approx 3.69$ ms for the equal mass, SR simulation in our work with use of the DD2 EOS. The leftmost and second-from-left panels depict the case where we assume the matter to consist of *npe* and *npe ν* matter, respectively. We highlight regions in the post-merger environment with rest mass density $\rho = 0.5\rho_{\text{sat}}$, ρ_{sat} , $2\rho_{\text{sat}}$, and $2.5\rho_{\text{sat}}$ (where $\rho_{\text{sat}} \approx 2.5 \times 10^{14}$ g cm⁻³ is the nuclear saturation density) using solid, dashed, dotted, and dash-dotted black lines, respectively. *Right:* Phase-space histograms for the two simulations depicted in the left panel. For these histograms we focus on a time window of ~ 3 ms before and after the merger. We mark the condition where $\mu_\Delta = T$ with solid black lines. Phase-space regions above (below) the solid lines where $T = \mu_\Delta$ imply that the matter is close to (significantly deviating from) weak equilibrium.

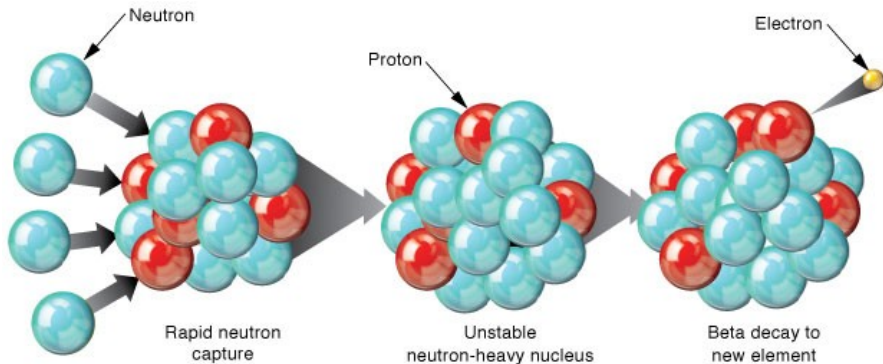
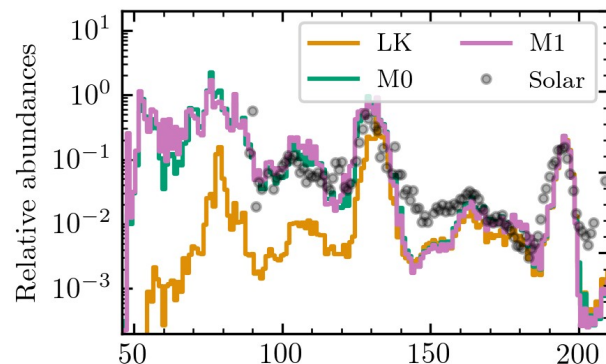
Dissipative effects, such as bulk viscosity, if present, are only active for a short window of time after the merger Espino+ [<https://arxiv.org/pdf/2311.00031>] (See also Perego+ [<https://arxiv.org/abs/1903.07898>])

Mass ejecta & nucleosynthesis

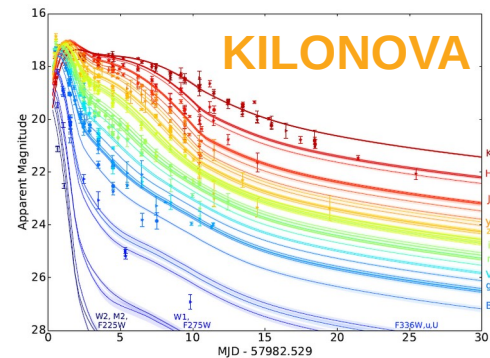


NS-BH collisions (1974) Decompression of cold neutron star matter

D. Schramm, J. Lattimer, D. Eichler, T. Piran, F. Thielemann, S. Rosswog and many others

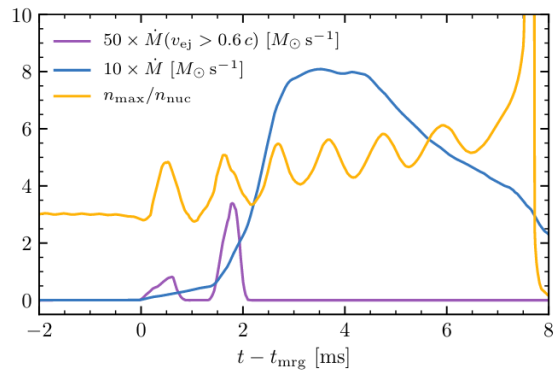
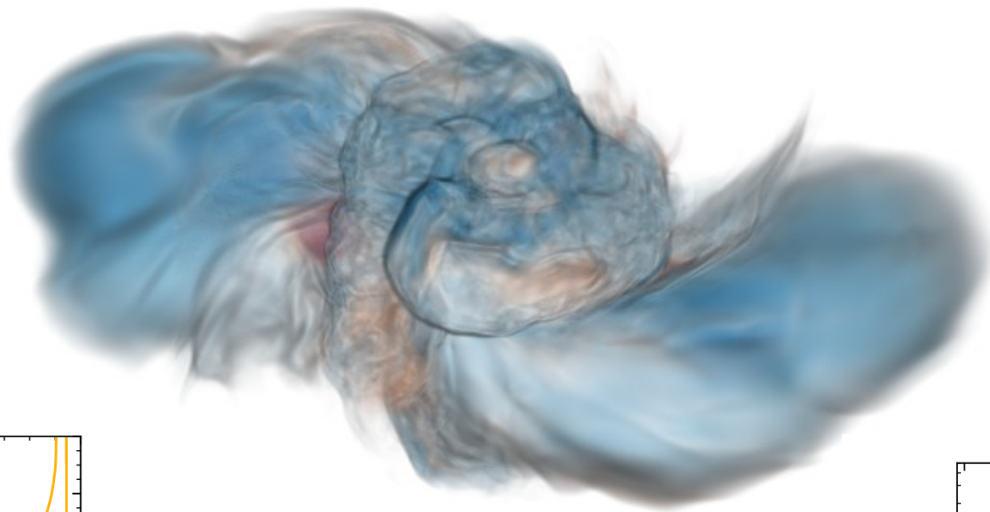


Radioactive heating & thermalization
(β -decays,
 α -decays, fission)



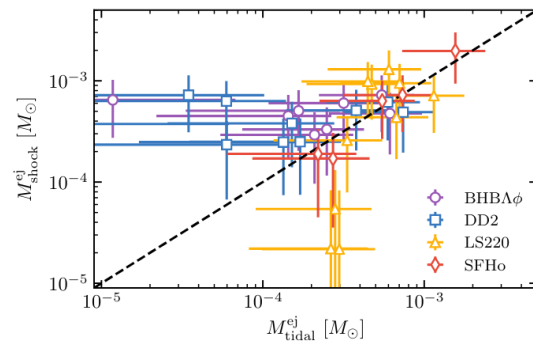
GW-driven phase: Dynamical ejecta

$$t - t_{\text{mrg}} = 0.6 \text{ ms}$$



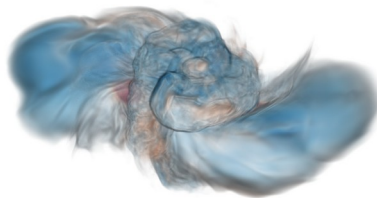
10 km

Radice+ [<https://arxiv.org/abs/1809.11161>]

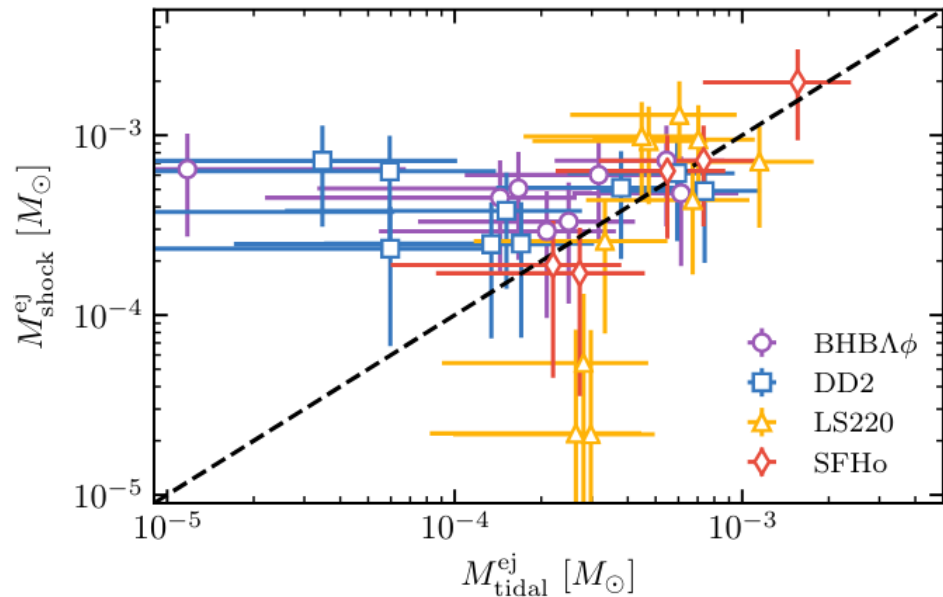
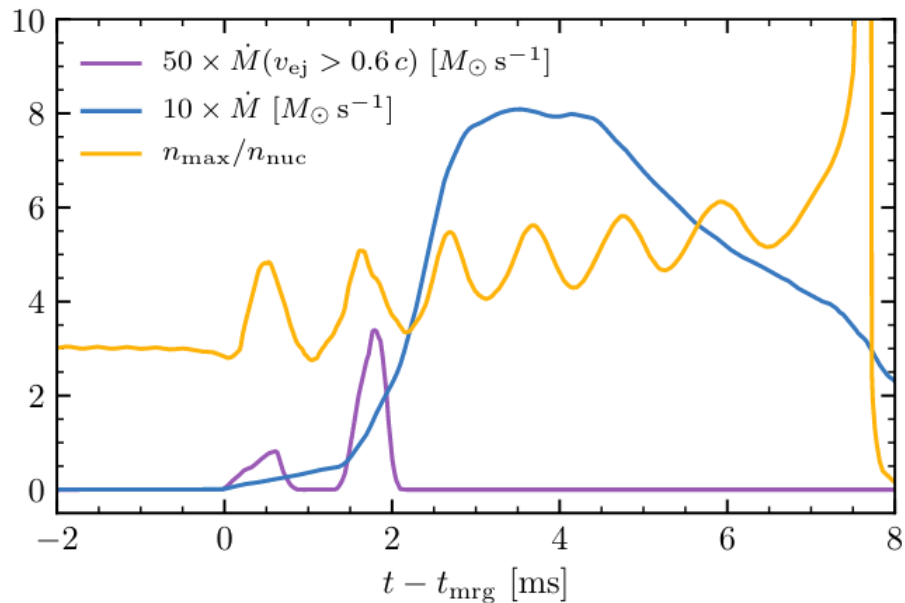


GW-driven phase: Dynamical ejecta

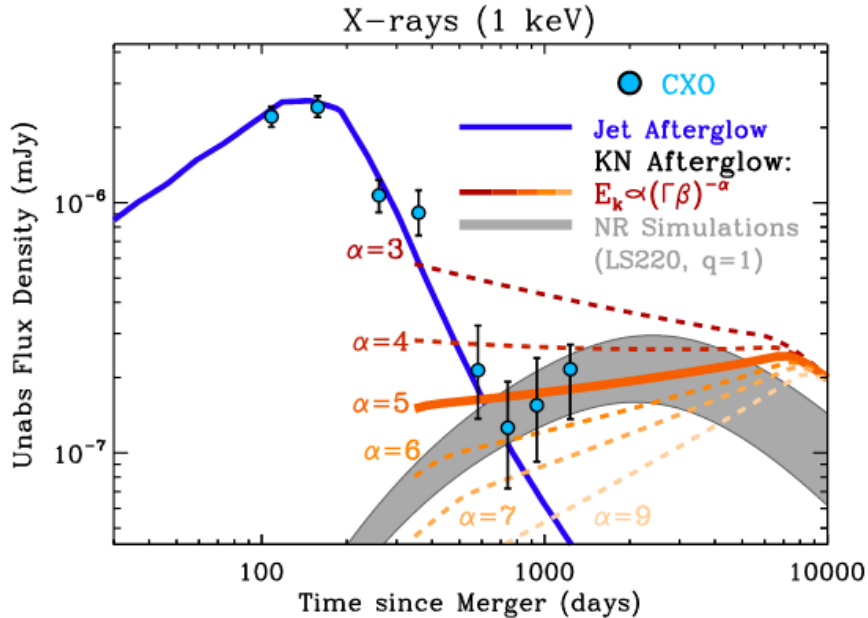
$t - t_{\text{mrg}} = 0.6 \text{ ms}$



10 km



X-ray rebrightening of GW170817?

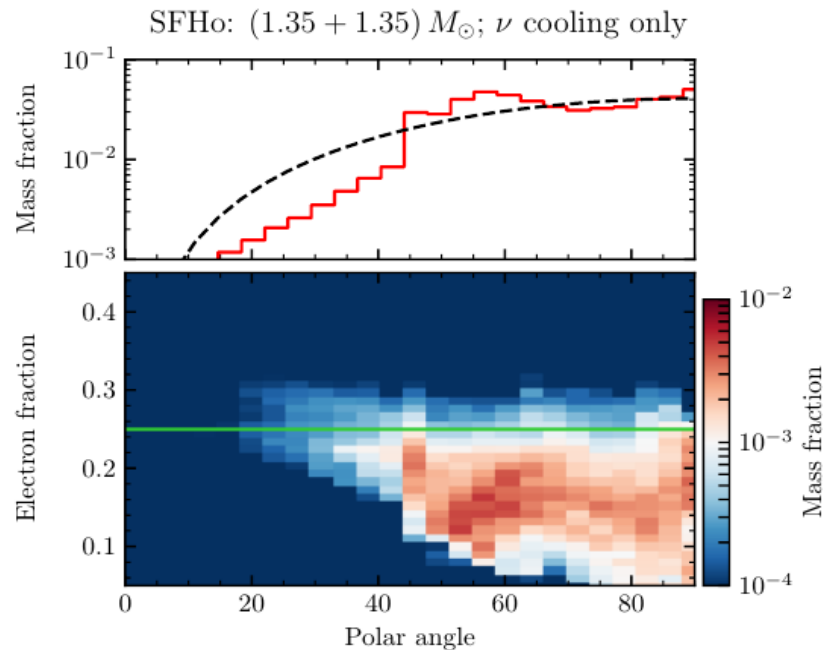
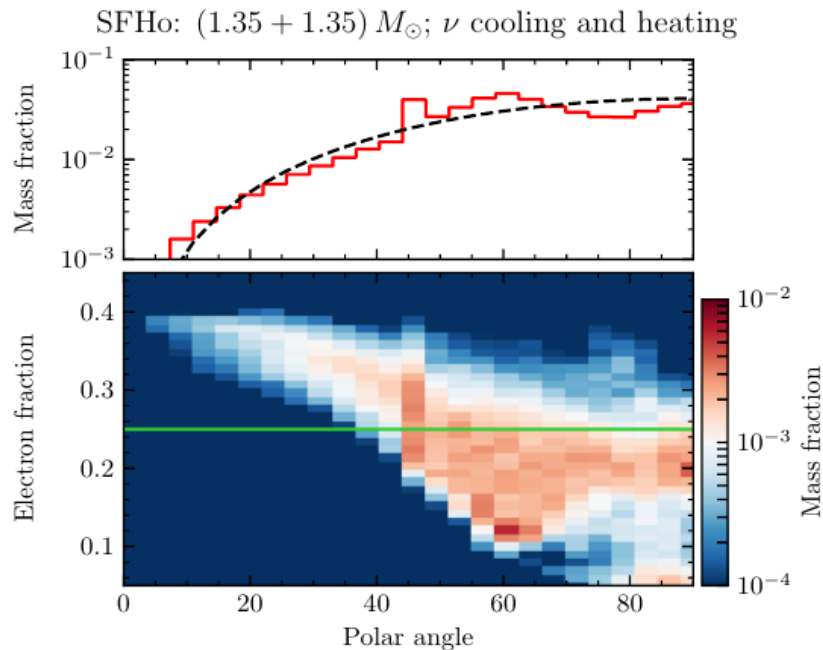


X-ray flux in excess to the expectations from the off-axis jet model 3 years after merger.

Consistent w/ **kilonova afterglow** due to high-speed ($\geq 0.6 c$) dynamical ejecta tails.

Possibility to constrain remnant and binary parameters.

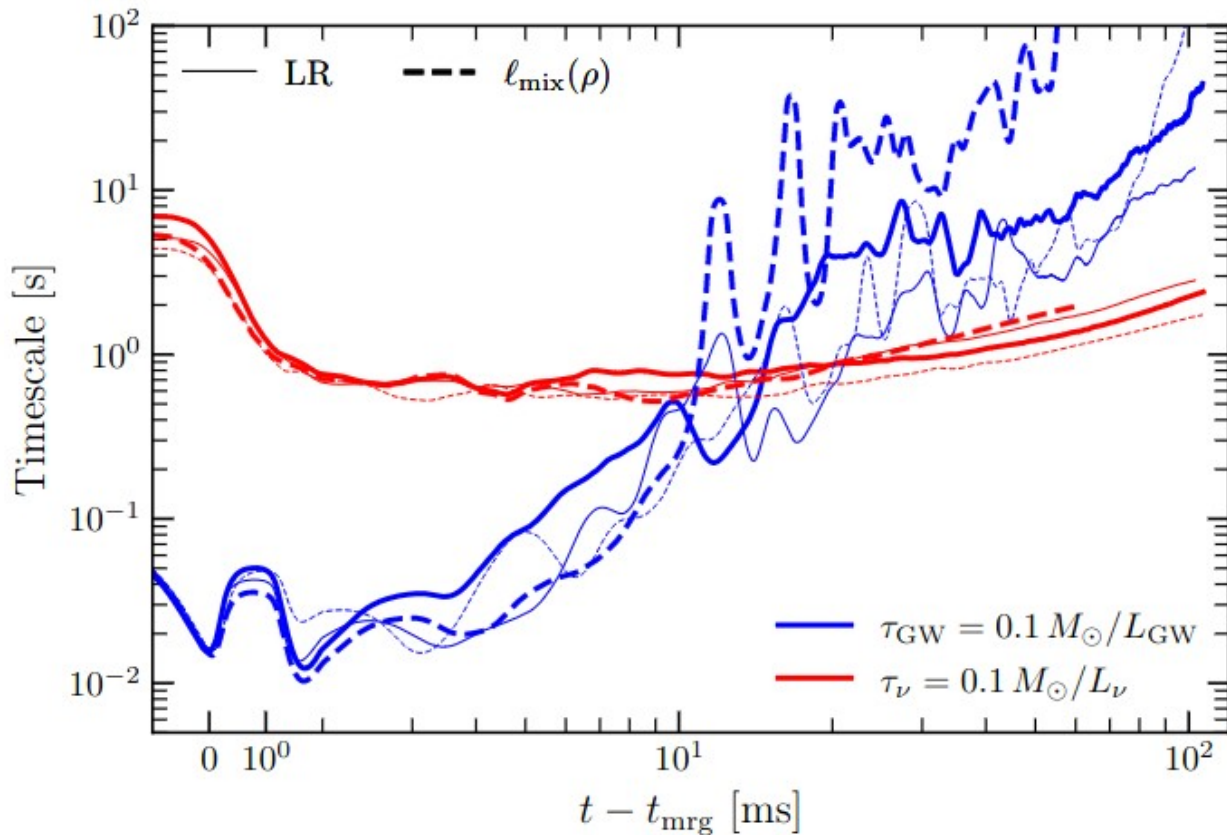
Weak interactions in the dynamical ejecta



Neutrino absorption determines both composition and kinetic properties !

[Perego,Radice,SB ApJL 2017] See also [Wanajo+ 2014, Sekiguchi+ 2016, Foucart+ 2017/2018]

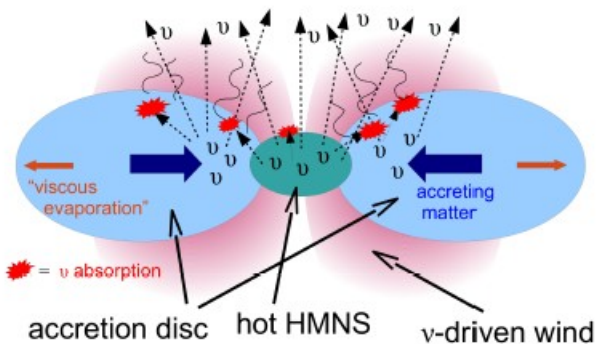
Viscosity-driven phase



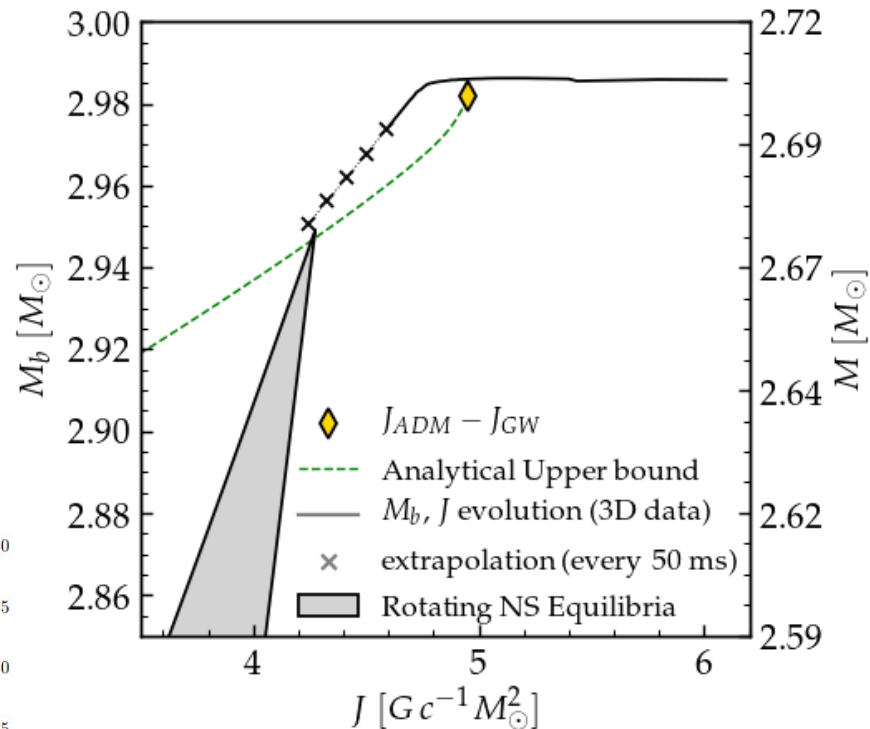
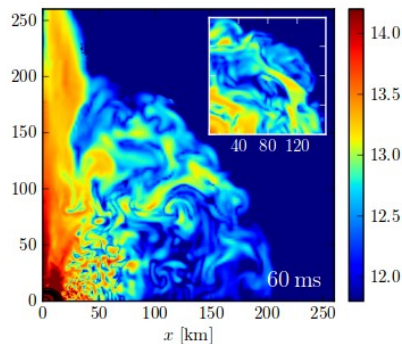
Remnants after the GW-driven phase

- Angular momentum (“super-Keplerian”) and mass in excess
- Evolution governed by neutrino cooling and viscous processes (magnetic turbulence & stresses, neutrino heating, etc)
- Discs $< \sim 0.1 M_{\odot}$: Nuclear recombination \rightarrow
Massive winds

[Perego+ 2014]

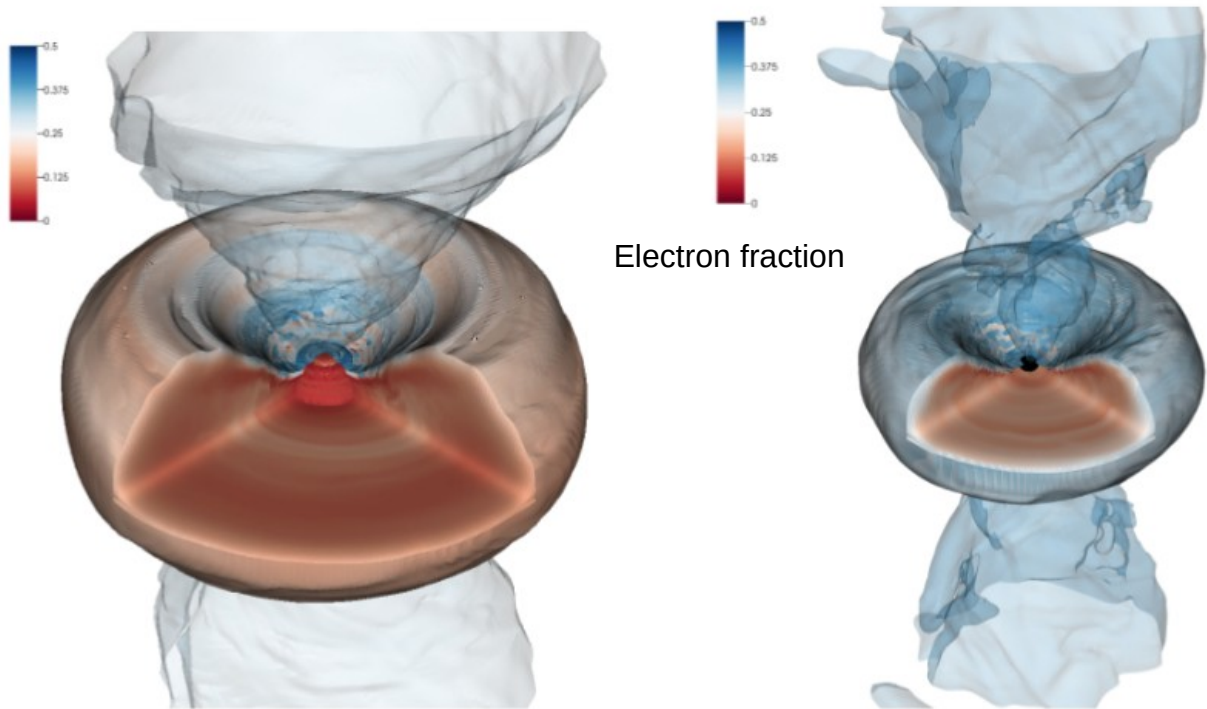


[Siegel+ 2014]



Radice, Perego, SB, Zhang [<https://arxiv.org/abs/1803.10865>]
Nedora, SB+ [<https://arxiv.org/pdf/2008.04333>]

Discs around NS and BH remnants



Perego, SB, Radice [<https://arxiv.org/abs/1903.07898>]

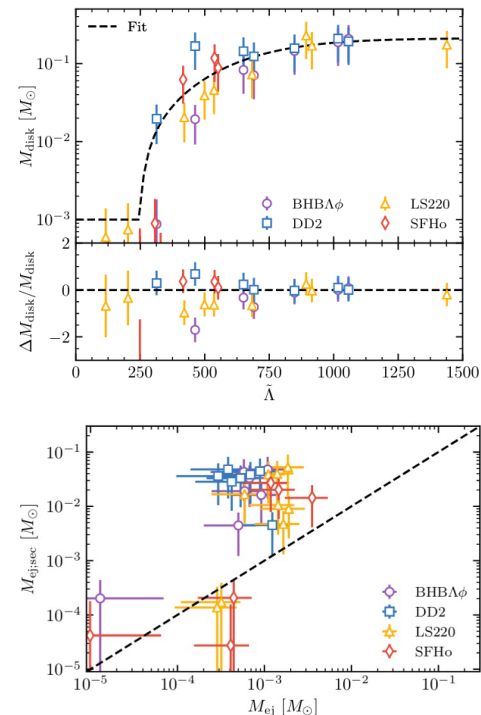
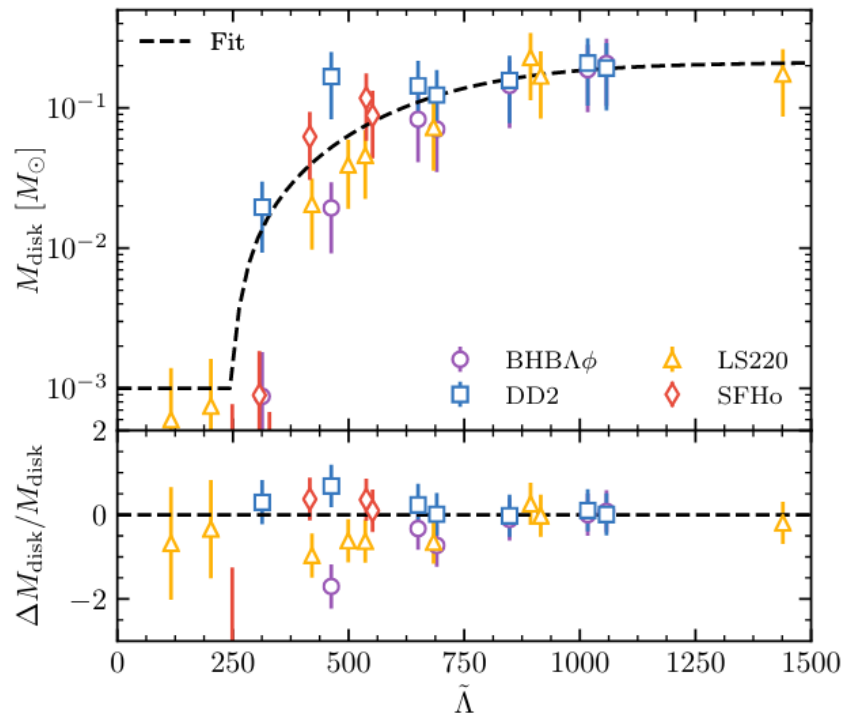
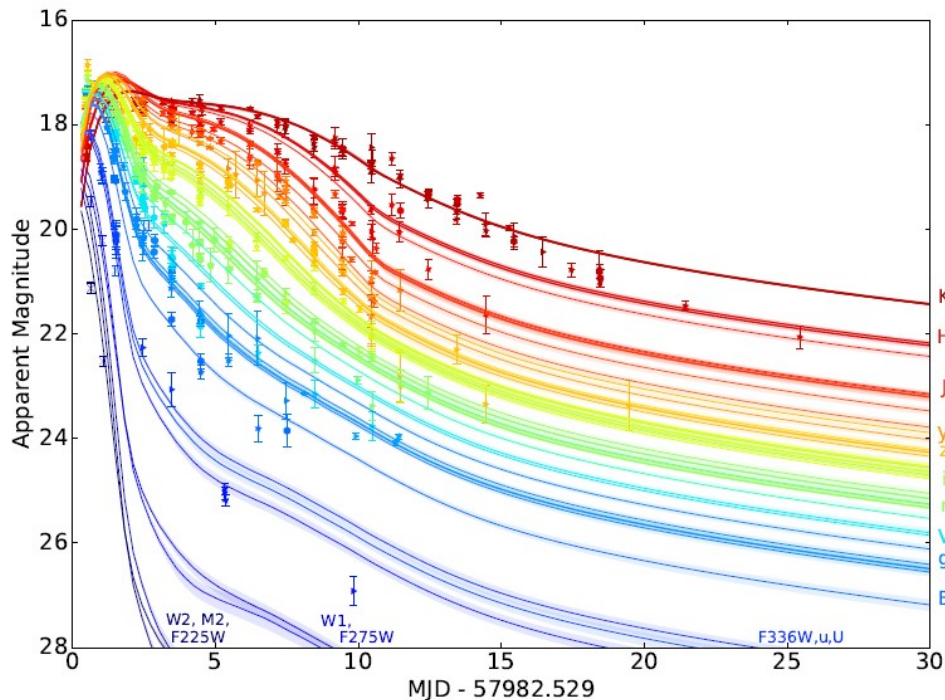


Figure 16. Dynamical ejecta $M_{\text{ej,dyn}}$ versus secular ejecta masses $M_{\text{ej,sec}}$. With the exception of the prompt BH formation cases that are able to expel at least a few $10^{-4} M_{\odot}$ in dynamical ejecta, the secular ejecta dominate over the dynamical ejecta.

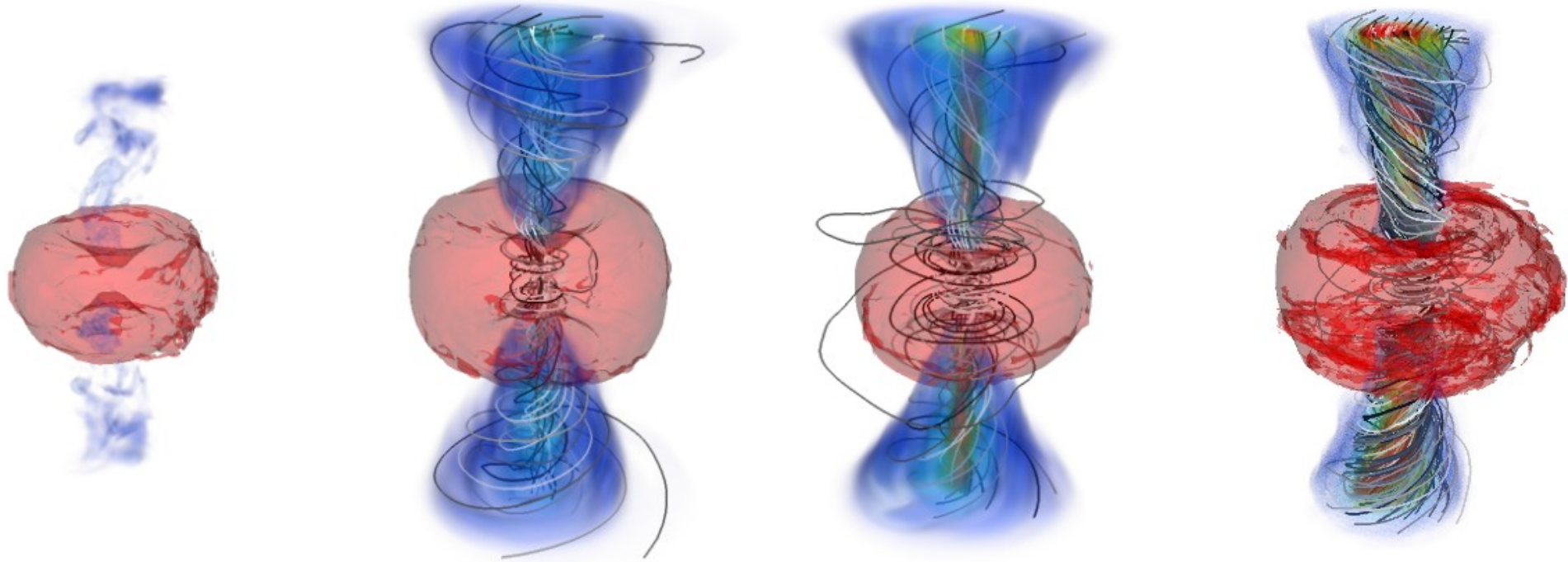
[<https://arxiv.org/abs/1809.11161>]

Mass, compactness, composition depends on binary parameters and central remnant
 Disc masses can be estimated from the reduced tidal parameter $\tilde{\Lambda}$ (EOS-insensitive relation)
 Disc winds significantly more massive than dynamical ejecta

AT2017gfo requires disk formation, and thus constrains the reduced tidal parameter



Jets from NS remnants

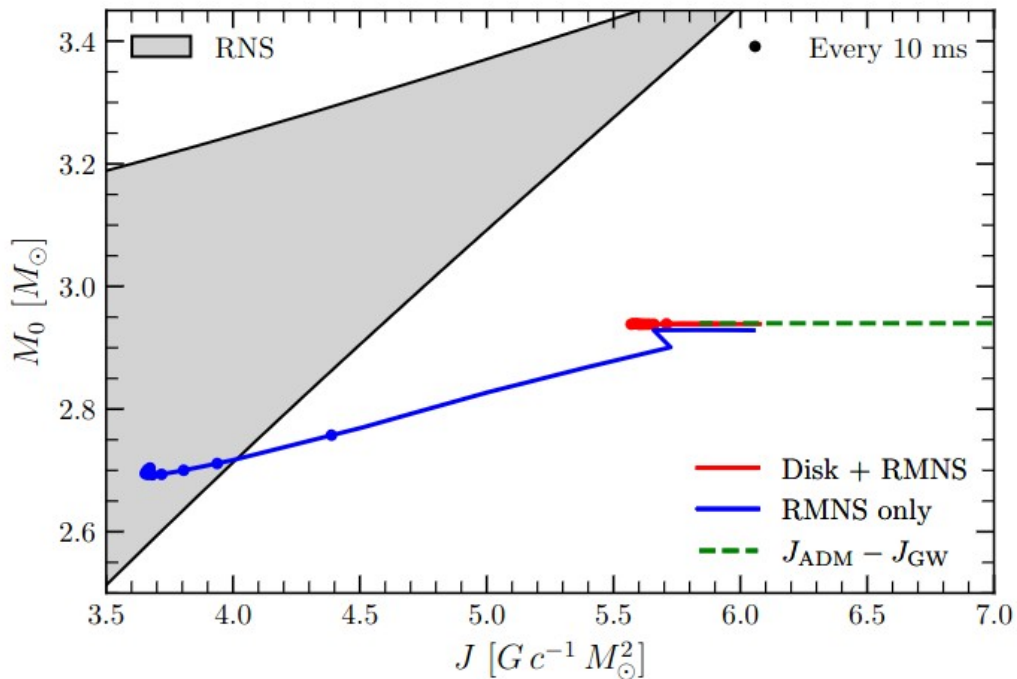


MRI (B-field amplification) + neutrino cooling (reduce baryon pollution)

Moesta et al [<https://arxiv.org/pdf/2003.06043>]

(Kenta's Talk yesterday!)

Long-lived NS Remnants



Ledoux criterion → remnant stably stratified → no convection
 Differential rotation persists w/ Omega peak at “surface”
 → core is MRI stable

Radice&SB [<https://arxiv.org/abs/2306.13709>]

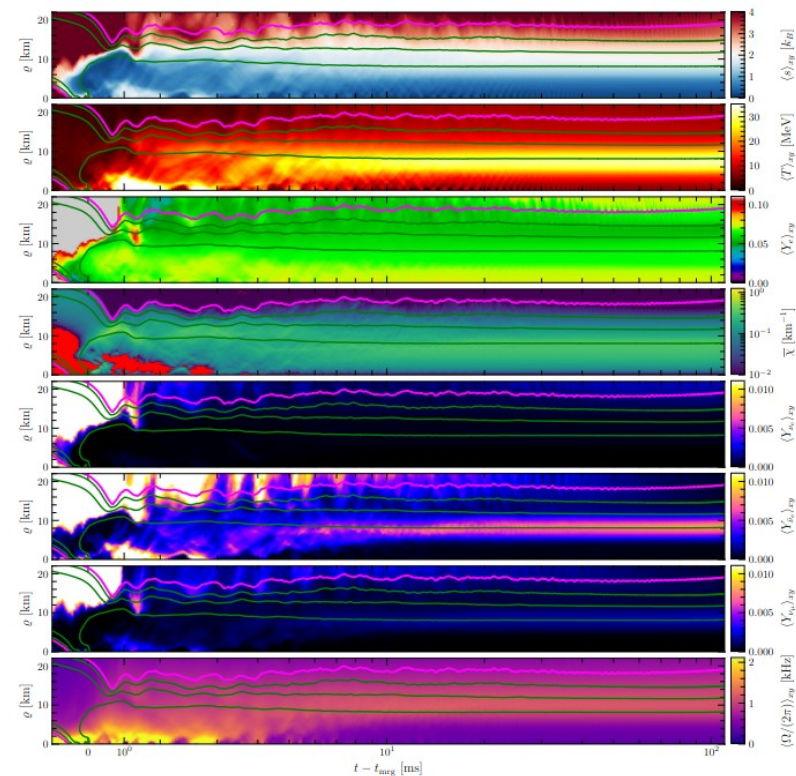
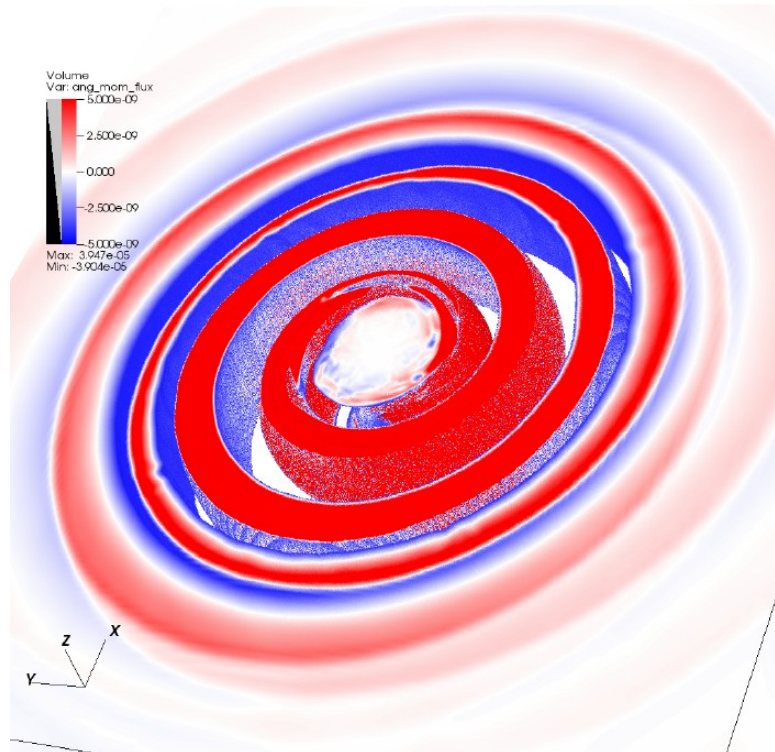


Figure 3. Angularly averaged profiles of entropy s , electron fraction Y_e , convection instability criterion χ , neutrino fractions Y_{ν_e} , Y_{ν_μ} , and Y_{ν_τ} , and angular frequency Ω on the equatorial plane for the $t_{\text{merg}} = 0$ SR binary. The profiles are shown as a function of cylindrical radius ρ and time from merger $t - t_{\text{merg}}$. The purple contour denotes $\rho = 10^{13.5}, 10^{14}$, and $10^{14.5} \text{ g cm}^{-3}$.

~100 ms 3D ab-initio evolutions with microphysics, M1 and GRLES (turbulent viscosity)

Long-lived Remnants: spiral-wave winds

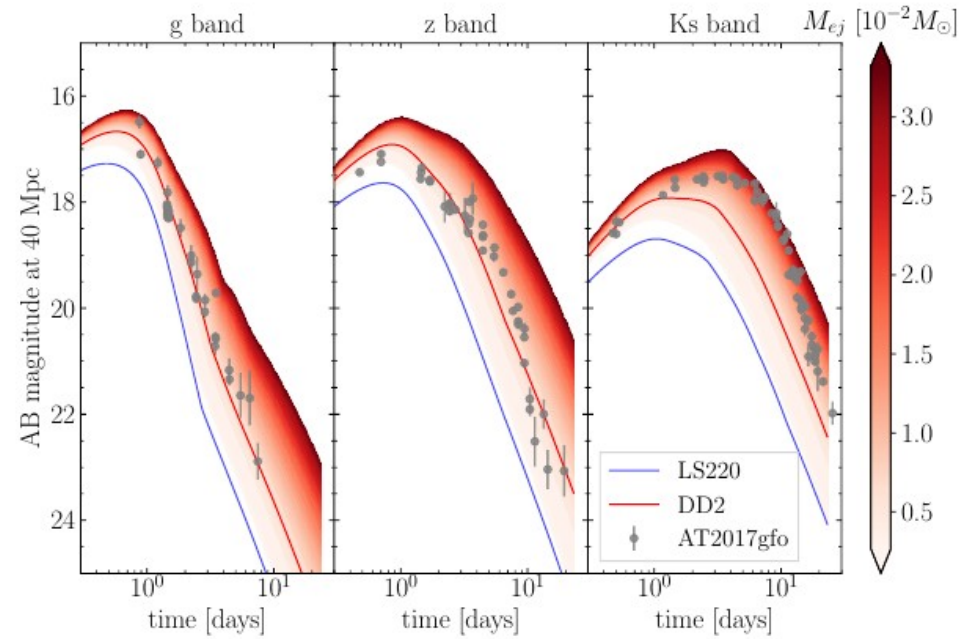


Nedora, SB+ [<https://arxiv.org/abs/1907.04872>]

Timescale ~ 10 s ms postmerger (to collapse)

Mass $\sim 0.01 M_{\odot}$ (to 100ms)

Generic mechanism boosted by neutrino heating/MHD component



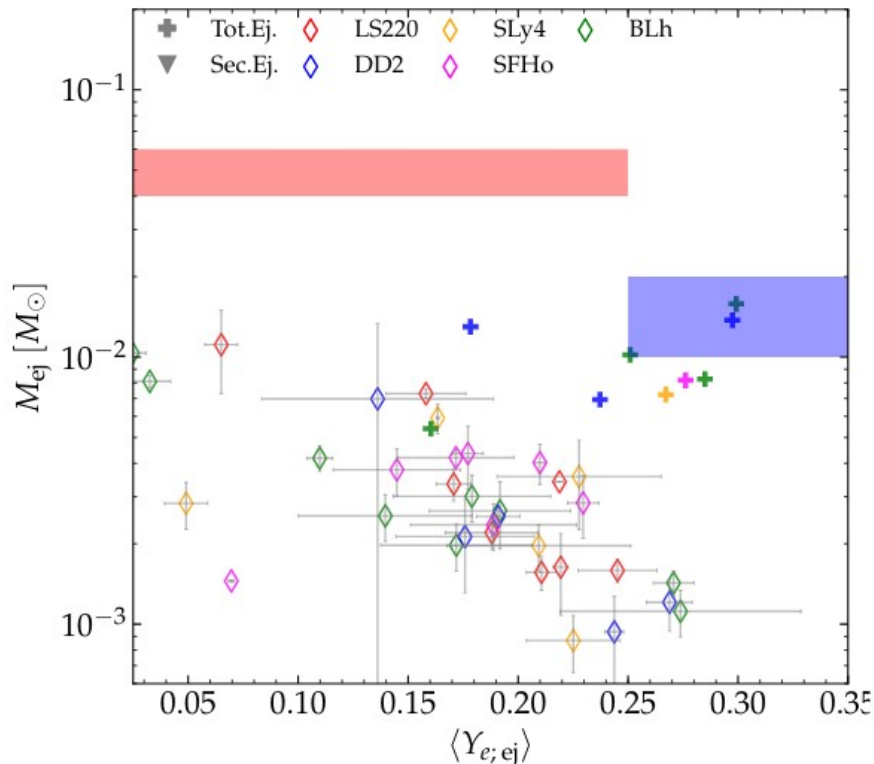
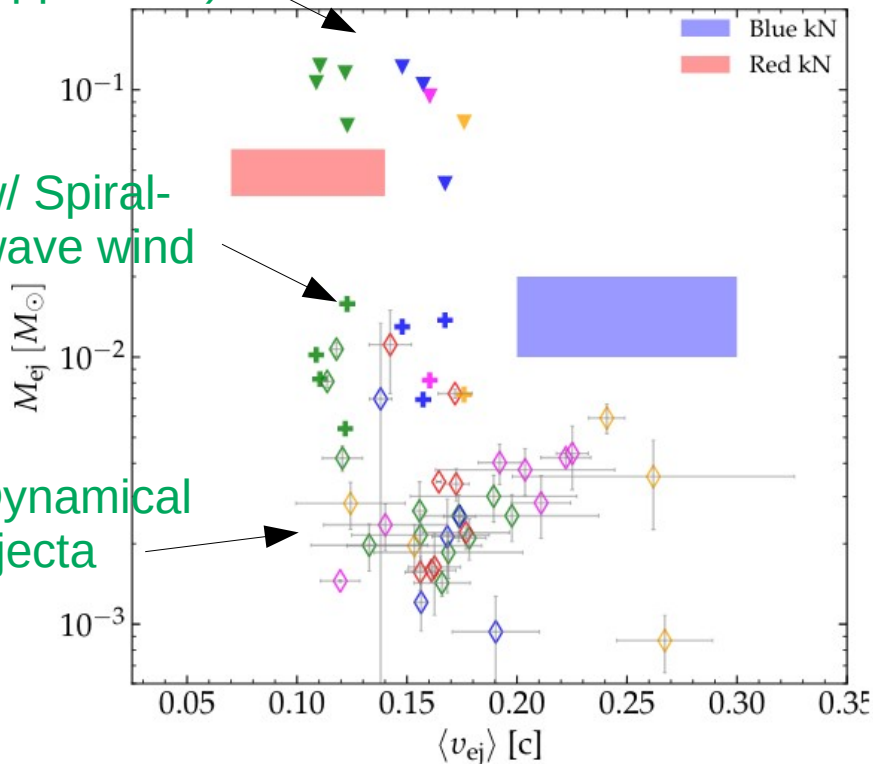
~ 100 ms 3D ab-initio evolutions with microphysics, M0 and GRLES (turbulent viscosity)

AT2017gfo & targeted simulations

Disc wind
(upper limit)

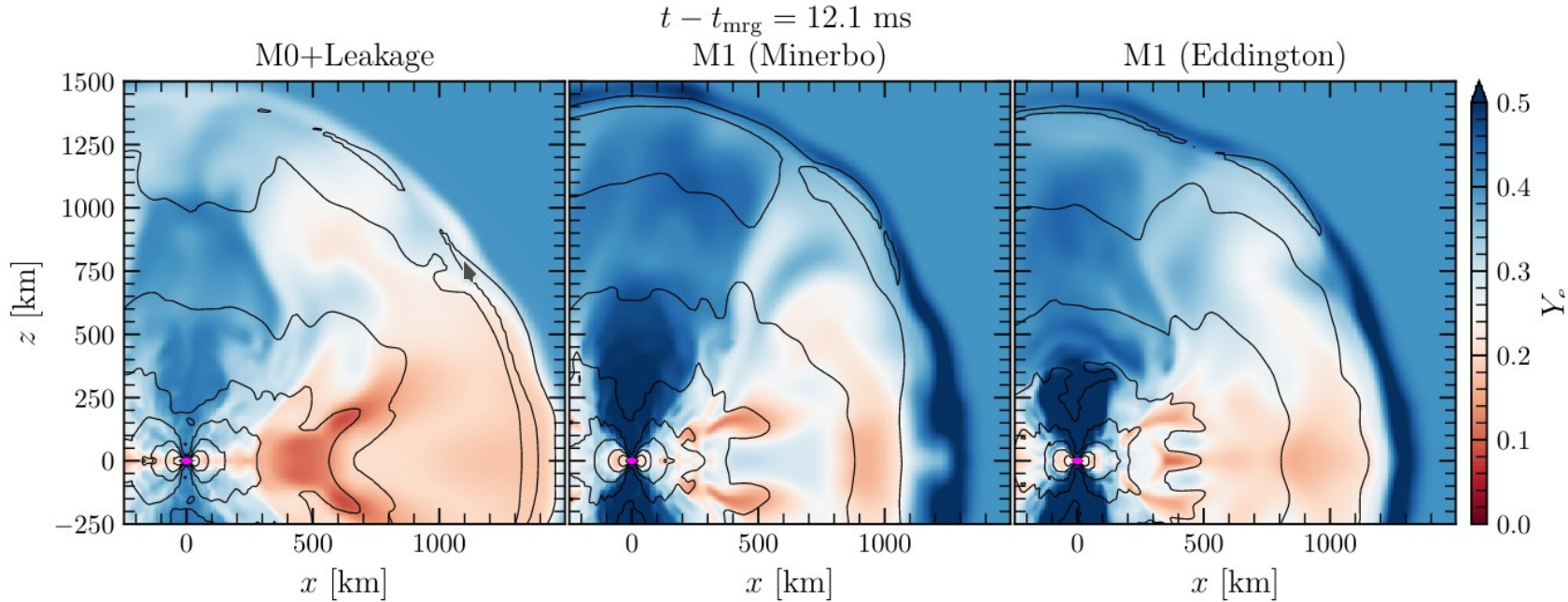
w/ Spiral-wave wind

Dynamical ejecta



Need at least two components high/low opacities (tentatively ~ dynamical ejecta+ winds ?)
Spherical two-component models are incompatible with NR ejecta

Impact of neutrino transport scheme



M1: neutrinos from RMNS (+50% energies; polar) and disc (larger area; equatorial) → increase Y_e differences and anisotropy

M1 (cf. M0): RMNS has neutrino trapped gas ($dT/T \sim$ - few %; Perego+ 2018); but no effects on GWs!

M1: Y_e close to equilibrium values above the remnant

M0 (cf. M1): transport happens only radially

M1 Eddington vs Minerbo: free streaming nus are slower $\sim 1/\sqrt{3}$ and interact further out

Impact of neutrino transport scheme

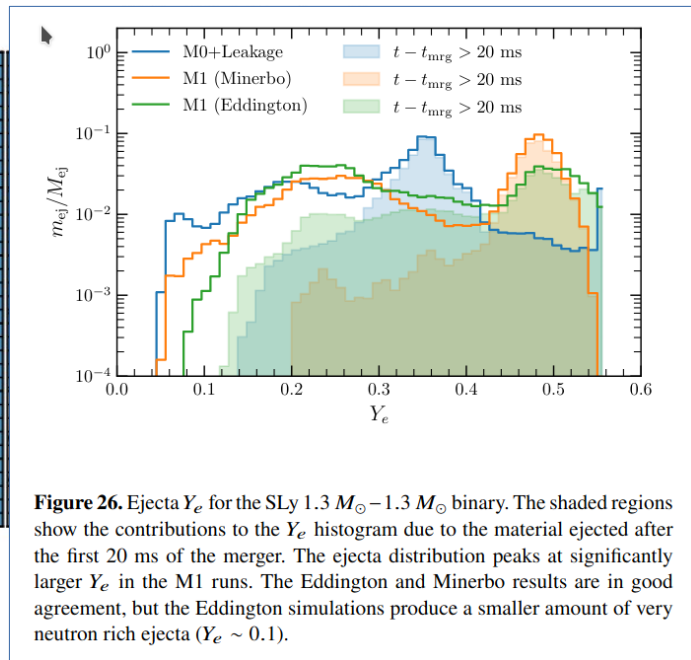
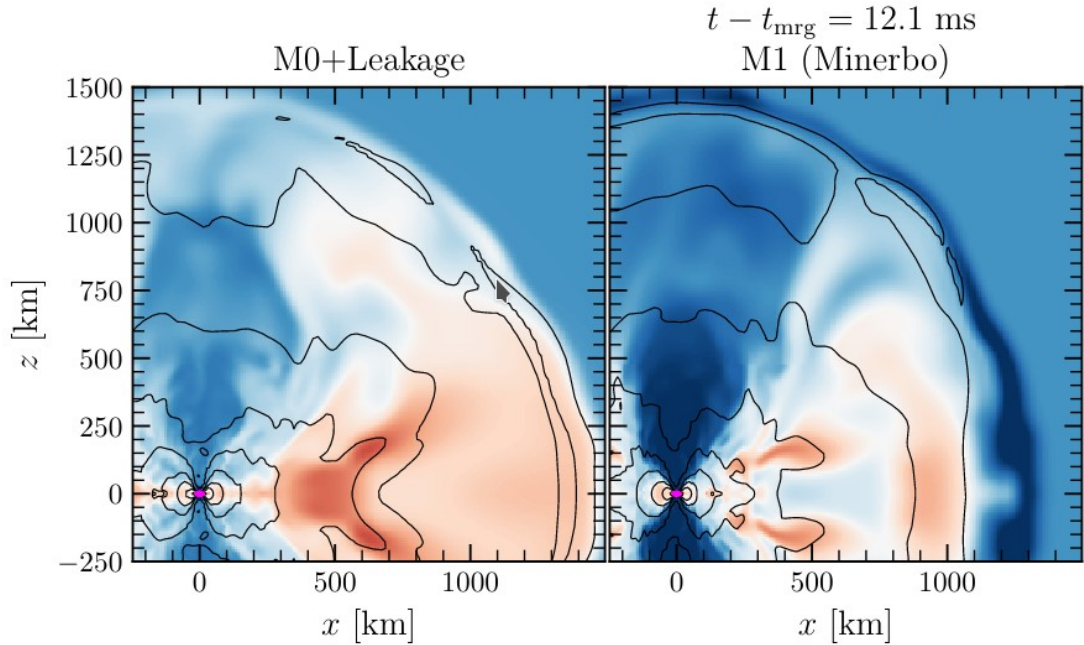


Figure 18. Electron fraction (color) of the dynamical ejecta cloud formed for the SLy $1.3 M_{\odot} - 1.3 M_{\odot}$ binary. The black lines are isodensity contours of $\rho = 10^5, 10^6, 10^7, 10^8, 10^9, 10^{10}, 10^{11}$, and $10^{12} \text{ g cm}^{-3}$. The purple contour shows corresponds to $\rho = 10^{13} \text{ g cm}^{-3}$ and denotes the approximate location of the surface of the merger remnant. M0 and M1 results are in good qualitative agreement, but M1 predicts higher electron fractions for both the polar and equatorial ejecta.

Yet another M1 gray+ scheme?!

Radice, SB, Perego, Haas 2021
[<https://arxiv.org/abs/2111.14858>]

Compare Foucart+ 2016 and Zelmani codes:

- Diffusion limit : 2nd order asymptotically preserving scheme.
Avoids ill-posed heat equation limit.
- complete matter-radiation sources:
Necessary even for simple tests

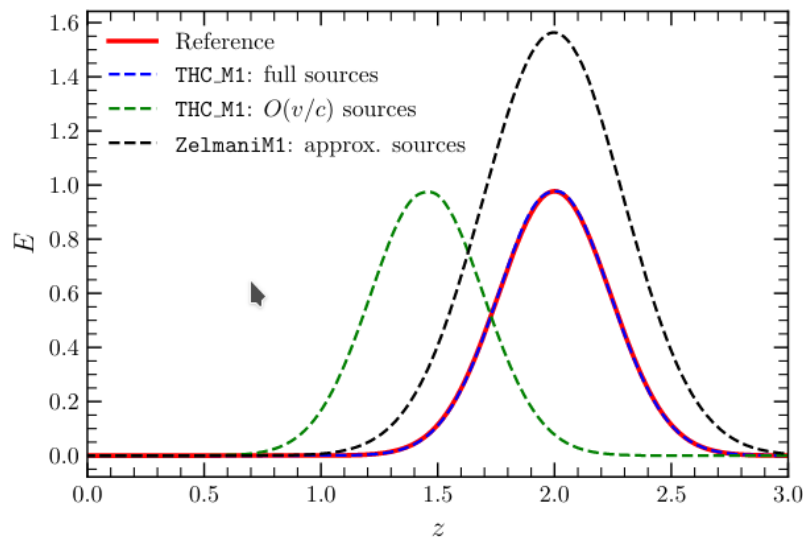
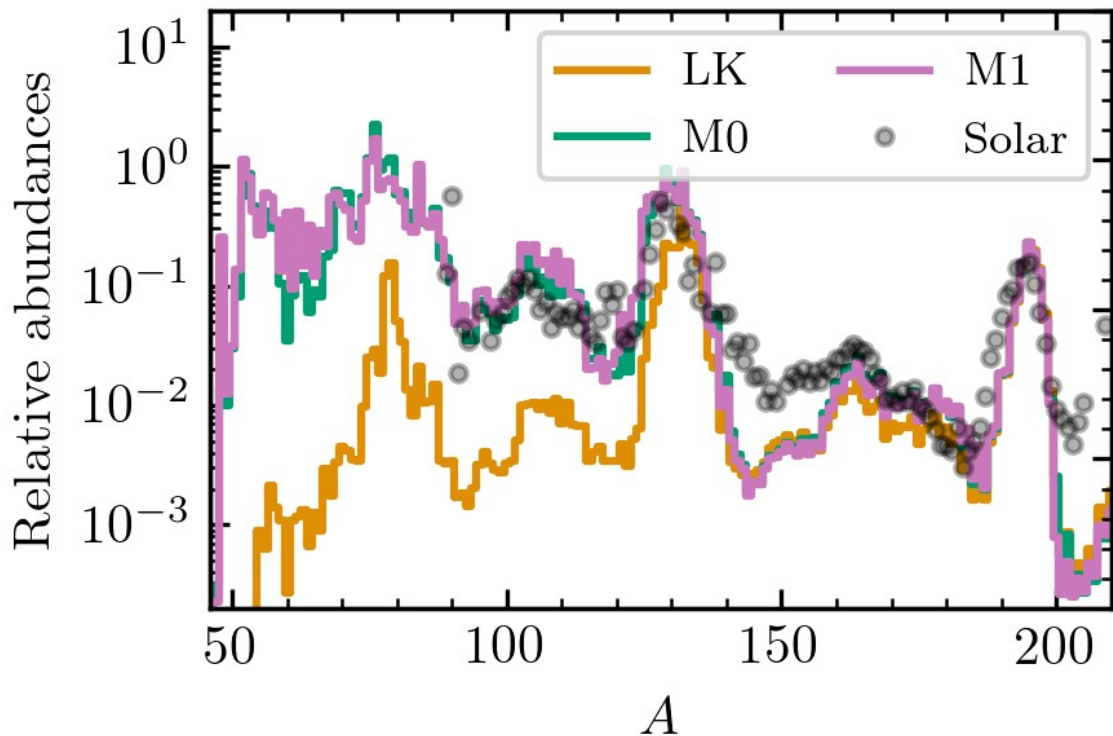


Figure 3. Diffusion and advection of Gaussian pulse of radiation in a purely scattering moving medium. The medium is moving with velocity $v = 0.5$. The reference profile is a translated semi-analytic solution of the diffusion equation. Our results show that it is essential to properly treat all of the source terms in the M1 equations to correctly capture the advection of trapped radiation.

Role of neutrino heating in nucleosynthesis

Systematic study of remnant and ejecta properties: neutrino schemes and mesh resolutions

Zappa, SB, Radice, Perego [<https://arxiv.org/abs/2210.11491>]

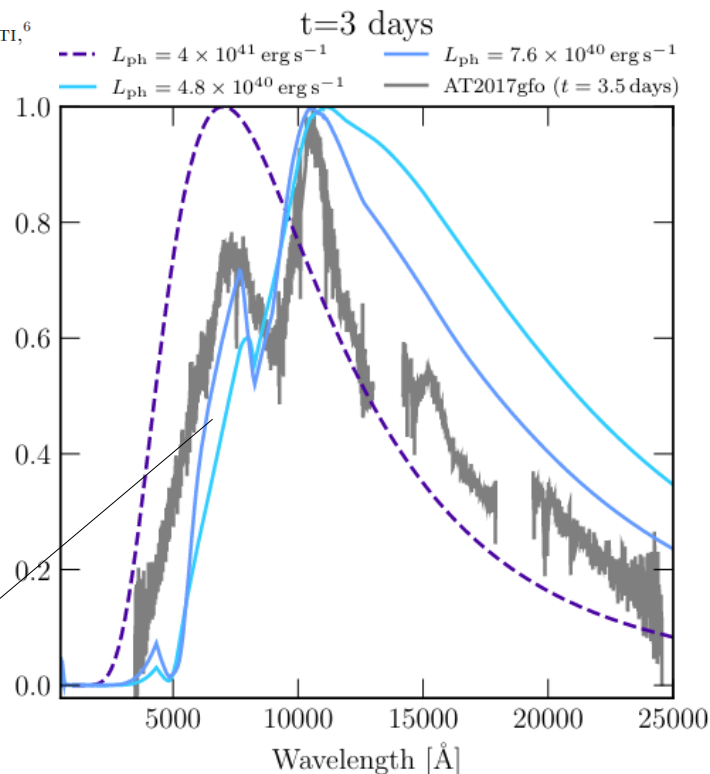
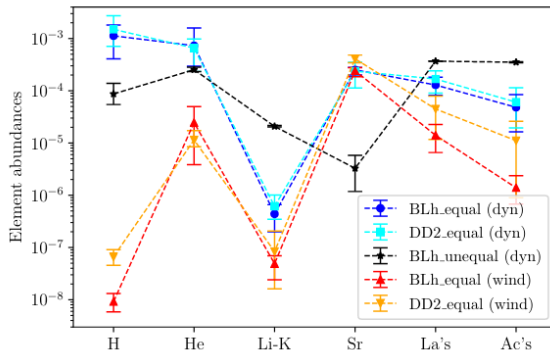
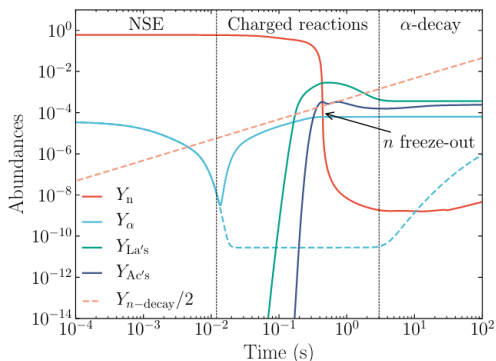


Gray M1 scheme with complete radiation-matter sources Radice,SB,Perego,Haas [<https://arxiv.org/abs/2111.14858>]

Ab-initio calculation of AT2017gfo spectra

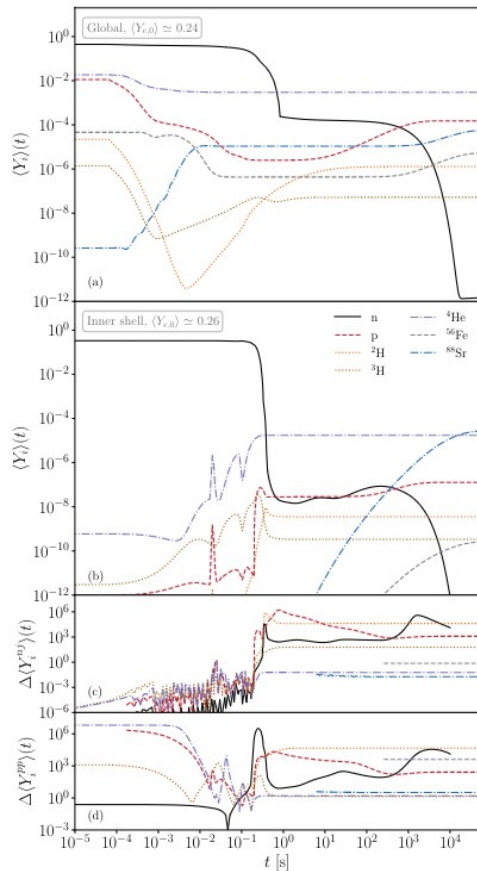
Production of very light elements and strontium in the early ejecta of neutron star mergers

ALBINO PEREGO,^{1,2} DIEGO VESCOVI,^{3,4,5} ACHILLE FIORE,^{6,7} LEONARDO CHIESA,¹ CHRISTIAN VOGL,^{8,9} STEFANO BENETTI,⁶
SEBASTIANO BERNUZZI,¹⁰ MARICA BRANCHESI,^{3,11} ENRICO CAPPELLARO,⁶ SERGIO CRISTALLO,^{5,4} ANDREAS FLÖRS,¹²
WOLFGANG E. KERZENDORF,^{13,14} AND DAVID RADICE^{15,16,17}



Reproduced Sr II feature identified in [Watson+ 2019](#)

Elements formation



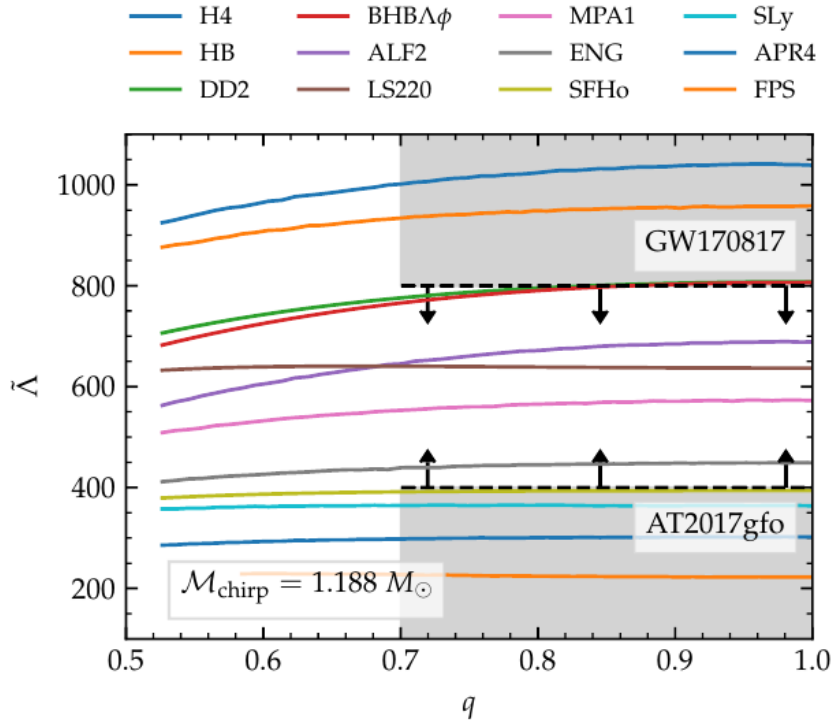
A first simulation of ejecta evolution with radiation-hydro and online nuclear network (2D ray-by-ray & SkyNet)

Nucleosynthesis yields are not accurately described by the initial thermodynamic profile of the ejecta

Abundancies show significant deviations when compared to the usual post-processing approach

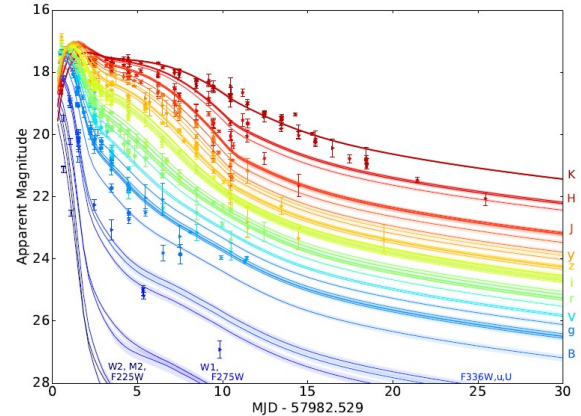
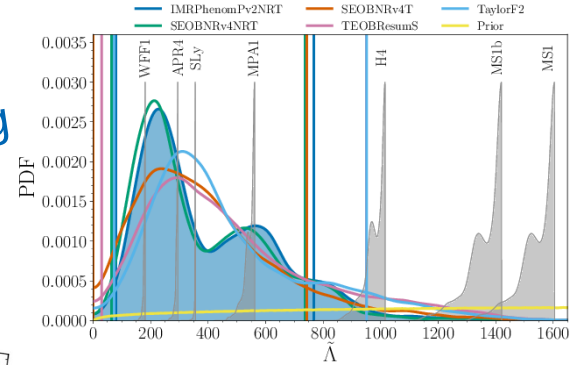
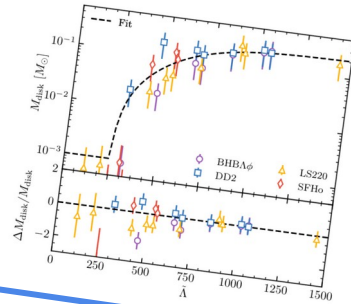
Coupling network-hydro can be relevant for quantitative predictions

Joint analyses to maximize science output

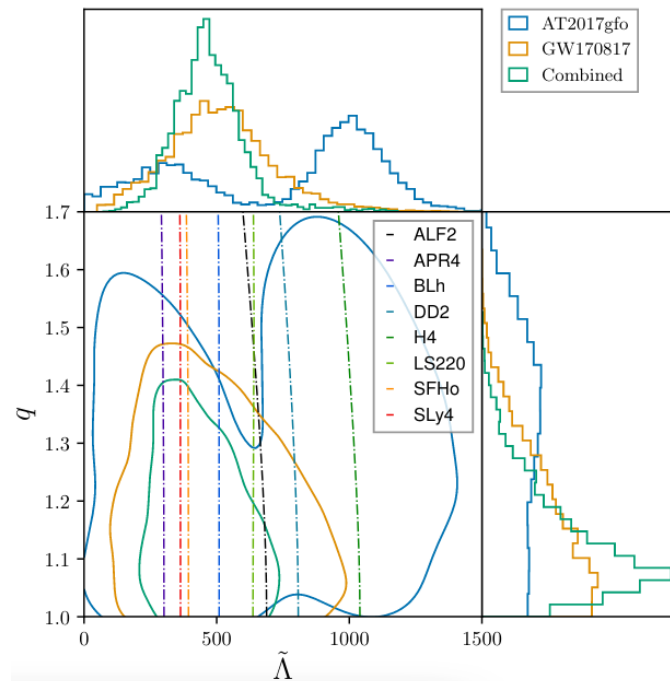
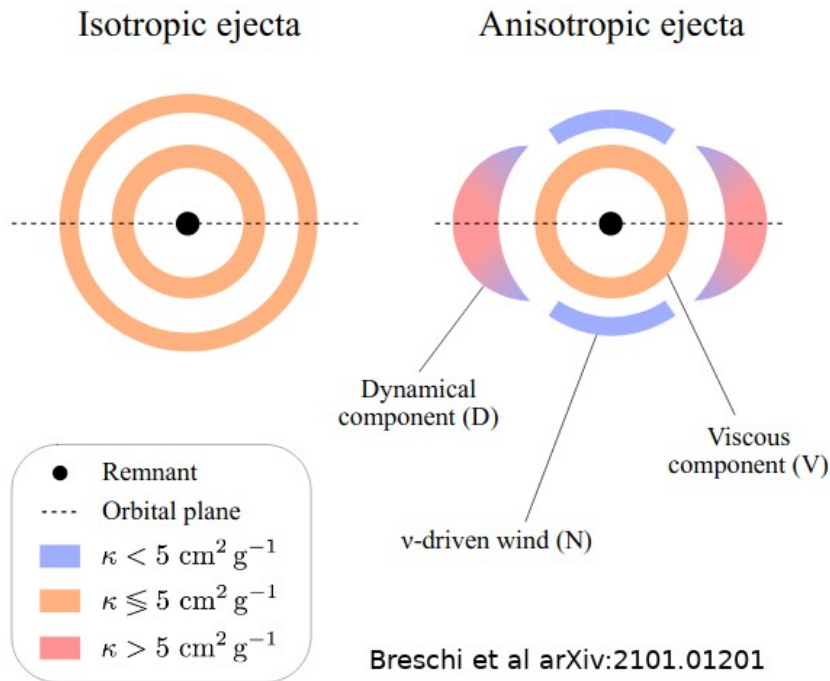


waveform modeling

simulations



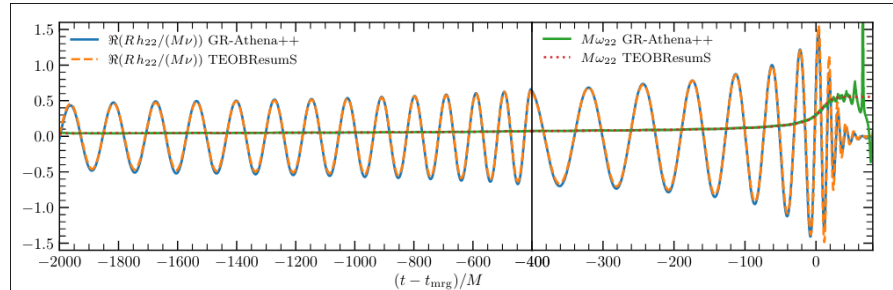
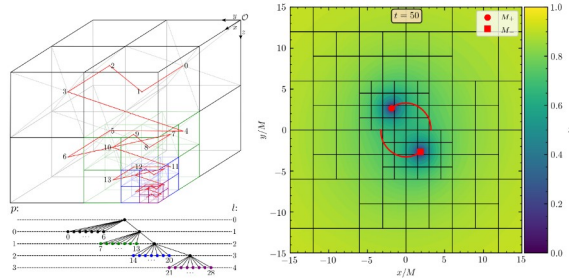
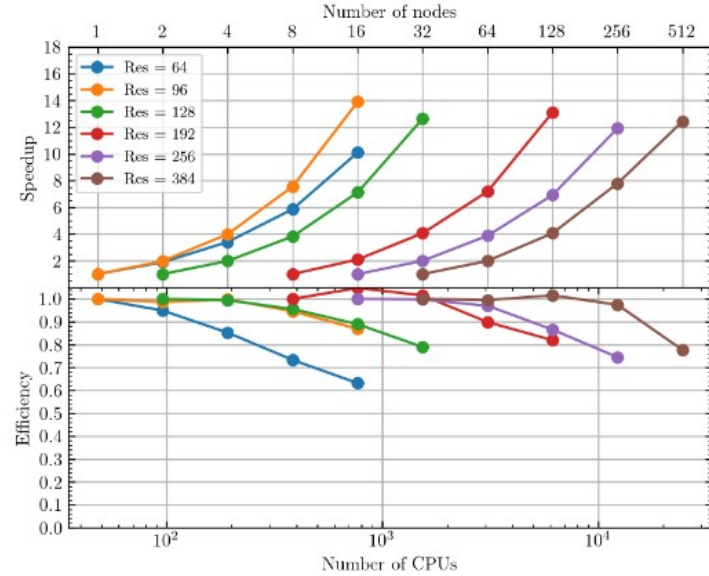
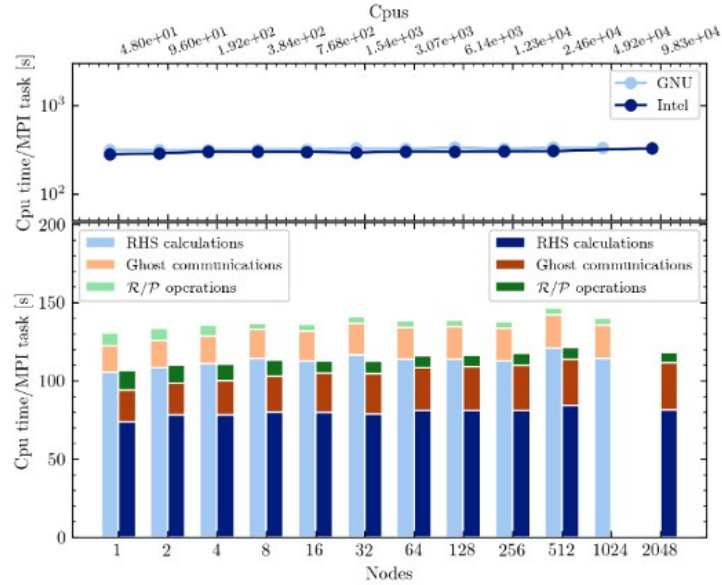
AT2017gfo Bayesian inference



Bayesian model selection: 3-components + anisotropic models preferred
Breschi+ [<https://arxiv.org/abs/2101.01201>]

Exascale numerical relativity

GR-Athena++ [Daszuta+ 2021, Cook+ 2023] based on Athena++ (Stone et al)



Conclusion

Complete gravitational-wave models for BNSM are essential to constrain NS matter via the measurement of tidal polarizability parameters and constraints on mass-radius diagram. Systematics are not under control at the precision required for measurements.

Next-generation detectors will be sensitive to postmerger (\sim kHz) GWs and physical effects in extreme matter (thermal, new d.o.f./phase transitions, etc) although an unambiguous procedure for the detection of such effects is not yet available.

NS remnant produced with angular momentum (“super-Keplerian”) and mass in excess \rightarrow massive winds developing on viscous timescales. NS remnants are stable against convection and MRI. Evolution to uniform rotation? How magnetic field breaks out of the star?

Neutrino transport impacts remnants, ejecta and nucleosynthesis (\rightarrow kilonova light curves.) Realistic simulations must include neutrino heating.

Simulations point to anisotropic, multi-component (different mechanisms) ejecta to explain AT2017gfo; they require, in particular, spiral-wave *and* disc winds. No simulation can yet quantitatively fit the observed data, although many features are nowadays explained.